NAVAL POSTGRADUATE SCHOOL
Monterey, California

THESIS

A DESCRIPTION OF TROPICAL CYCLONE
RECURVATURE IN TERMS OF
ISENTROPIC POTENTIAL VORTICITY

by

Andrew P. Boerlage

June 1989

Thesis Advisor	Russell L. Elsberry

Approved for public release; distribution is unlimited.

90 02 :? 013

security classification of this page

REPORT DOCUMENTATION PAGE

1a Report Security Classification Unclassified		1b Restrictive Markings			
2a Security Classification Authority		3 Distribution Availability of Report			
2b Declassification Downgrading Schedule		Approved for public release; distribution is unlimited.			
4 Performing Organization Report Number(s)		5 Monitoring Organization Report Number(s)			
6a Name of Performing Organization Naval Postgraduate School	6b Office Symbol (if applicable) 35	7a Name of Monitoring Organization Naval Postgraduate School			
6c Address (city, state, and ZIP code) Monterey, CA 93943-5000		7b Address (city, state, and ZIP code) Monterey, CA 93943-5000			
8a Name of Funding Sponsoring Organization	8b Office Symbol (if applicable)	9 Procurement Instrument Identification Number			
8c Address (city, state, and ZIP code)		10 Source of Funding Numbers			
		Program Element No	Project No	Task No	Work Unit Accession No

11 Title (include security classification) A DESCRIPTION OF TROPICAL CYCLONE RECURVATURE IN TERMS OF ISENTROPIC POTENTIAL VORTICITY

12 Personal Author(s) Andrew P. Boerlage

13a Type of Report Master's Thesis	13b Time Covered From To	14 Date of Report (year, month, day) June 1989	15 Page Count 70

16 Supplementary Notation The views expressed in this thesis are those of the author and do not reflect the official policy or position of the Department of Defense or the U.S. Government.

17 Cosati Codes			18 Subject Terms (continue on reverse if necessary and identify by block number)
Field	Group	Subgroup	Isentropic Potential Vorticity, Bogus Vortex Structure

19 Abstract (continue on reverse if necessary and identify by block number)
Isentropic potential vorticity (IPV) fields calculated from the Navy Operational Regional Atmospheric Prediction System are analyzed to determine their usefulness as an aid to tropical cyclone recurvature forecasts. The IPV fields associated with Typhoon Nelson are calculated on a 80 km grid for the period 0000 UTC 4 October to 0000 UTC 7 October 1988. In this preliminary study, IPV advection fields and the horizontal and vertical structure of the bogus vortex are examined to determine their contributions to the model forecast. The extremely broad bogus vortex is found to distort the IPV fields and cause regions of negative IPV, which is believed to result in inertial instability. Approximately 36 h are required for the model to adjust to the initial imbalance in the mass and wind fields. It appears that the unrealistic bogus vortex representation may have degraded the early portions of the model forecast. Analysis of IPV advection fields each 12 h during the NORAPS model integration showed that storm movement is primarily due to the influence of self-advection and the large-scale steering flow. During later periods other advective features associated with adjacent synoptic systems begin to influence the storm movement. Forecasters with access to such IPV fields may be able to evaluate the likely validity of the model forecast of recurvature. The usefulness of the IPV representation from the NORAPS prediction in this single case study suggest that additional cases of tropical cyclone recurvature be examined in terms of IPV concepts. Theses

20 Distribution Availability of Abstract ☒ unclassified unlimited ☐ same as report ☐ DTIC users	21 Abstract Security Classification Unclassified	
22a Name of Responsible Individual Russell L. Elsberry	22b Telephone (include Area code) (408) 646-2044	22c Office Symbol 64?

DD FORM 1473,84 MAR   83 APR edition may be used until exhausted   security classification of this page
All other editions are obsolete

i

A description of tropical cyclone
recurvature in terms of
isentropic potential vorticity

by

Andrew P. Boerlage
Captain, United States Air Force
B.S., Washington State University, 1981

Submitted in partial fulfillment of the
requirements for the degree of

MASTER OF SCIENCE IN METEOROLOGY

from the

NAVAL POSTGRADUATE SCHOOL
June 1989

Author: _____
Andrew P. Boerlage

Approved by: _____
Russell L. Elsberry, Thesis Advisor

_____
Wendell A. Nuss, Second Reader

_____
Robert J. Renard, Chairman,
Department of Meteorology

_____
Gordon E. Schacher,
Dean of Science and Engineering

ABSTRACT

Isentropic potential vorticity (IPV) fields calculated from the Navy Operational Regional Atmospheric Prediction System are analyzed to determine their usefulness as an aid to tropical cyclone recurvature forecasts. The IPV fields associated with Typhoon Nelson are calculated on a 80 km grid for the period 0000 UTC 4 October to 0000 UTC 7 October 1988. In this preliminary study, IPV advection fields and the horizontal and vertical structure of the bogus vortex are examined to determine their contributions to the model forecast. The extremely broad bogus vortex is found to distort the IPV fields and cause regions of negative IPV, which is believed to result in inertial instability. Approximately 36 h are required for the model to adjust to the initial imbalance in the mass and wind fields. It appears that the unrealistic bogus vortex representation may have degraded the early portions of the model forecast. Analysis of IPV advection fields each 12 h during the NORAPS model integration showed that storm movement is primarily due to the influence of self-advection and the large-scale steering flow. During later periods other advective features associated with adjacent synoptic systems begin to influence the storm movement. Forecasters with access to such IPV fields may be able to evaluate the likely validity of the model forecast of recurvature. The usefulness of the IPV representation from the NORAPS prediction in this single case study suggest that additional cases of tropical cyclone recurvature be examined in terms of IPV concepts.

TABLE OF CONTENTS

v

LIST OF TABLES

LIST OF FIGURES

ACKNOWLEDGEMENTS

I. INTRODUCTION

Tropical cyclones, which account for the strongest sustained winds observed, pose an extreme hazard to military and civilian operations. Inaccurate forecasts of the movement of these storms have led to loss of life and resources. According to Elsberry (1987), tropical cyclone forecasts have improved relative to the 1960's in terms of reducing error magnitude as well as in terms of consistency. Long-term forecasts (48 to 72 h) have the greatest errors, especially for storms that have erratic tracks and for those that recurve. Elsberry (1987) states that track errors associated with an incorrect assessment of the recurvature situation may exceed 1850 km (1000 n mi) at 72 h. Because the impact of these forecasts is usually very high, it is essential that techniques be developed to improve recurvature forecasts.

An accurate long-term forecast is critical for military operations. The time required to secure or deploy resources to prevent damage due to high winds is beyond the time period when the most success has been achieved in tropical cyclone forecasting. An inaccurate long-term forecast can have very costly consequences. Loss of life, aircraft and mission readiness may result from these deficiencies.

The goal of this study is to demonstrate the utility of potential vorticity fields during the recurvature of tropical cyclones as they interact with midlatitude cyclones. Isentropic potential vorticity (IPV) fields associated with both the tropical and midlatitude cyclone are analyzed to determine if the orientation and advection of these fields with respect to the two systems may be a precursor for the recurvature of the tropical cyclone.

IPV fields have provided a useful description of extratropical cyclogenesis (Hoskins et al. 1985). Other researchers (Uccellini et al. 1985) have made use of IPV fields to describe explosive cyclogenesis. Normally, IPV would not be considered relevant in the quasi-barotropic tropics. However, the important interactions with extratropical systems during recurvature may be described well in terms of IPV lobes approaching the tropical cyclone such that the advection of IPV accounts for the deflection of the tropical cyclone into the midlatitudes.

Just as the sparsity of observations has hindered studies of maritime extratropical cyclones, the lack of observations also impedes the use of IPV in the tropics. Availability of data only at the mandatory pressure levels, and thus only poor vertical resol-

1

ution, has made it extremely difficult to describe accurately the vertical structure of IPV in tropical cyclones. Researchers have overcome these hurdles by utilizing various models. Schubert and Alworth (1987) and Thorpe (1985) make use of analytical models to describe IPV structures associated with the tropical cyclone vortex. The use of numerical models in determining the vertical structure of IPV in extratropical cyclones has been handicapped due to the lack of vertical resolution (Elsberry and Kirchoffer 1988).

This study describes IPV features using a a research version of the Navy Operational Regional Atmospheric Prediction System (NORAPS). NORAPS has an advantage over other models in that its horizontal (80 km) and vertical (21 levels) resolution should be sufficient to describe accurately the small-scale features. Thus, an analysis of the NORAPS data should show interaction between the midlatitude and tropical cyclone. Typhoon Nelson, the only super-typhoon of the 1988 season, was selected because it was accurately forecast by NORAPS. The results of this study may facilitate the use of operational IPV analysis and hopefully allow the forecaster to evaluate the 48 and 72 h forecasts of recurving tropical cyclones.

Chapter II summarizes past research with IPV fields. Chapter III describes the synoptic situation during the recurvature of Nelson and also summarizes the NORAPS forecast of this storm. A description of Typhoon Nelson in terms of IPV fields is presented in Chapter IV. This chapter also includes a section on the advection of potential vorticity and how this may affect the propagation of the storm. Appendix A gives an indepth description of the NORAPS model, and Appendix B outlines the procedures for the calculation of potential vorticity from the NORAPS fields. Conclusions and suggestions for further study are outlined in Chapter V.

II. BACKGROUND

The significance of potential vorticity (PV) and its effect on meteorological phenomena cannot be over-emphasized. Within the last 10 years, researchers have attempted to explain such phenomena as cyclogenesis and explosive cyclogenesis in terms of the distribution and structure of PV in the atmosphere. Hoskins *et al.* (1985) provide a historical perspective for a number of early studies concerning the details and upper-air structure of PV.

1. Midlatitude applications

The conservative properties of PV make it an ideal tracer of air parcels in the atmosphere. Reed (1955) and Reed and Sanders (1953) made use of this concept to distinguish air that is of stratospheric origin from tropospheric air due to the large values of PV normally found in the stratosphere. The greater thermal stability of the stratosphere provides for the high values of PV. Shapiro (1980) confirms the application of this concept in his calculations of PV on isentropic surfaces from aircraft observations of jet streams.

Reed (1955) applied the PV tracer by demonstrating that stratospheric air could be advected down sloping isentropic surfaces to altitudes well within the troposphere. This injection of stratospheric air into the tropopause is defined as a tropopause fold. This phenomenon is a mechanism for detaching stratospheric air with high values of PV and transporting this air toward the mid-troposphere along the axis of the jet. Reed suggested that there is a link between the tropopause fold and upper-level frontogenesis. Danielsen (1968) confirmed Reed's hypothesis and stated that the large values of PV normally observed in upper-level fronts are of stratospheric origin. Tropopause folds usually occur to the west of developing troughs along the axis of confluence separating the thermodynamic direct and indirect circulation cells beneath the core of the jet (Danielsen 1968). Upper-level fronts that are located in the negative vorticity region between the trough and the upstream ridge are located in a region of downward motion where the strongest subsidence occurs near the warm edge of the front. The sinking of warm air intensifies the temperature gradient due to adiabatic compression. In his study of a midlatitude cyclone, Shapiro (1980) concluded that intense baroclinic processes within and on the scale of upper-level fronts are a key factor in extratropical cyclogenesis.

3

Uccellini *et al.* (1985) propose that the high values of isentropic potential vorticity (IPV) found in the tropopause fold and associated with the upper-level front may be a possible triggering mechanism for the explosive development of extratropical cyclones. They suggest that cyclogenesis could occur as stratospheric air with high values of PV is injected into the troposphere, and the vortex tubes are then stretched as the static stability decreases significantly. If the high values of stratospheric PV are to be conserved then the absolute vorticity must increase, which will enhance the cyclonic circulation in the troposphere. If this upper-level vorticity maximum is superposed on a region of low-level baroclinity, cyclogenesis may occur.

Uccellini *et al.* (1985) demonstrate that the injection of high values of PV into the lower levels of the troposphere may have been a triggering mechanism for the explosive development of Presidents' Day cyclone of 18-19 February 1979. They show that the high values of PV were advected over the storm center when explosive cyclogenesis occurred. They concluded that the explosive development of the cyclone was enhanced by the descent of stratospheric air and the extension of high potential vorticity to lower levels.

Although the usefulness of IPV fields for understanding the structure and behavior of mid-latitude weather systems has been demonstrated, operational use of IPV fields has been hampered by various factors (Elsberry and Kirchoffer 1988). Before the advent of computers, the extra computational time needed to create isentropic analysis relative to isobaric analysis was a hindrance. The second factor is the need for significant level data to accurately define the positions and magnitudes associated with features such as tropopause folds, inversions and other stable layers. This restriction is critical for maritime analysis where few rawinsondes exist. The lack of observations hinders the use of the IPV tools in conjunction with tropical cyclone structure. To overcome this inhibiting factor, researchers have used numerical and analytical models. Operational numerical models do not have adequate vertical resolution to describe key IPV features. Numerical models may not realistically represent all of the physical processes involved.

2. Tropical cyclone application

Various analytical models have been used to simulate the vortex structure of tropical cyclones in terms of PV. Thorpe (1985) uses PV concepts in extending quasi-geostrophy and semi-geostrophy to balanced curved flows. His equation set consists of a prognostic equation for the PV and two diagnostic equations for the potential function

4

$$\Phi = \phi + \frac{v^2}{2},$$

where ϕ is the geopotential and v is the gradient wind. These equations give the balanced vortex structure and an equation for the agradient circulation produced by diabatic forcing. Thorpe (1985) indicates that the vortex structure is completely determined at any given time by the solution of the potential function equation, if the boundary variations of potential temperature and the interior variation of PV are known. He concludes that the variations in PV can occur either in association with a sloping tropopause or in the troposphere due to diabatic heating that produces both sources and sinks of PV. A tropopause that descends over the vortex produces a negative radial gradient of PV that is consistent with cyclonic flow. This phenomena would counteract the tendency for upper anticyclonic circulation due to the warm core structure of the tropical cyclone. He determined that the inclusion of a tropopause in the model also increased the low-level cyclonic flow. Conversely, a tropopause that is elevated in the core is consistent with anticyclonic flow. Thorpe's first attempts to describe PV structure in a tropical cyclone using an analytical model proved to be the starting point for other researchers.

Schubert and Alworth (1987) also make use of an analytical model in their description of the evolution of PV in tropical cyclones. They solve Eliassen's (1952) balanced vortex equations analytically so that the value of PV is known at all times. Making use of the "invertibility principle" as described by Hoskins *et al.* (1985), they diagnostically deduce the complete flow structure of the tropical cyclone from the spatial distribution of PV. Their numerical results indicate that latent heat release produces a region of large PV in lower levels and a region of small PV at upper levels. Due to vertical advection, the upper tropospheric minimum is pinched off as large PV spreads throughout the troposphere. This configuration causes tangential winds to develop at an increasing rate, so that typhoon strength winds are attained within 96 h. If the PV is allowed to continue to evolve, intense low-level winds are produced.

Schubert and Alworth (1987) and Thorpe (1985) introduce a somewhat different view of tropical cyclones with primary attention focused on the PV field. Since PV fields are very significant in midlatitude baroclinic waves and frontogenesis, researchers have moved closer to the goal of unified dynamical framework for the study of midlatitude and tropical cyclones.

The lack of high-resolution observations is a great problem in determining the structure of IPV in tropical cyclones. Earlier studies used analytical models to overcome these resolution problems. This study attempts to represent the IPV structure in a tropical cyclone and a midlatitude cyclone during recurvature by using numerical model output. The Navy Operational Regional Atmospheric Prediction System (NORAPS) output fields are selected to describe the key upper-level features because of its increased vertical resolution.

Comparisons of key IPV structures is the goal of this study. As mentioned by Hoskins *et al.* (1985), IPV maxima associated with stratospheric air in the tropopause fold is a key feature in the upper-level cyclone whereas a maximum (minimum) of IPV is expected in the low levels (upper levels) of the tropical cyclone. Therefore, it is expected that an interaction due to the IPV gradients should occur as the tropical cyclone moves poleward. This study attempts to show that the interaction of the two lobes of IPV and how they are oriented in relation to the two systems may be a precursor in forecasting the recurvature of a tropical cyclone.

III. SYNOPTIC DISCUSSION AND FORECAST TRACK OF TYPHOON NELSON

A. SYNOPTIC DISCUSSION

Typhoon Nelson was the first major tropical cyclone in the western North Pacific during October 1988. A lull in tropical cyclone activity had occurred in the later part of September as polar air pushed southward across the Asian mainland and Japanese Islands. During this period, the monsoon trough had returned to its normal position. Nelson developed in the monsoon trough over the Philippine Sea and initially moved toward the west and then northwest as it tracked along the periphery of the subtropical ridge. Nelson intensified as it moved to the northwest and reached peak winds of 140 kt (72 m/s) at 1200 UTC 4 October. By 0000 UTC 5 October, Nelson had begun to re-curve (Fig. 1). As will be described below, the synoptic situation during this time period was ideal for recurvature to the northeast. An upper-level trough located between the stationary Tibetan High and the subtropical high over the western Pacific deflected Nelson to the northeast. The relatively stationary large-scale features controlling the motion probably contributed to an accurate forecast of Nelson's recurvature (to be discussed below).

Key aspects of the synoptic evolution that relate to the movement and the inter-action with a midlatitude cyclone are highlighted in the next section. Two levels are selected for analysis. The upper level (300 mb) provides an accurate description of the interaction of Nelson with the midlatitude cyclone, whereas the midlevel (500 mb) is selected to represent the steering flow. Although considerable debate still exists as to which level or layer most accurately represents the tropical cyclone movement, a high correlation exists between tropical cyclone displacement and the flow at the mid-tropospheric levels. Elsberry (1987) states that the best representation may be a deep-layer mean flow that would include winds of 850, 700, 500, 400 and 250 mb. In this case, an adequate description can be achieved with the 500 mb winds.

NOGAPS analysis in the immediate region of the typhoon is suspect due to the lack of observations. Key typhoon features, such as upper-level cyclonic flow near the center and a transition to anticyclonic flow at larger radius, are not described and must be bogused into the analysis. The analysis is also limited in horizontal resolution. Small-scale features occurring during the interaction of the typhoon with the midlatitude
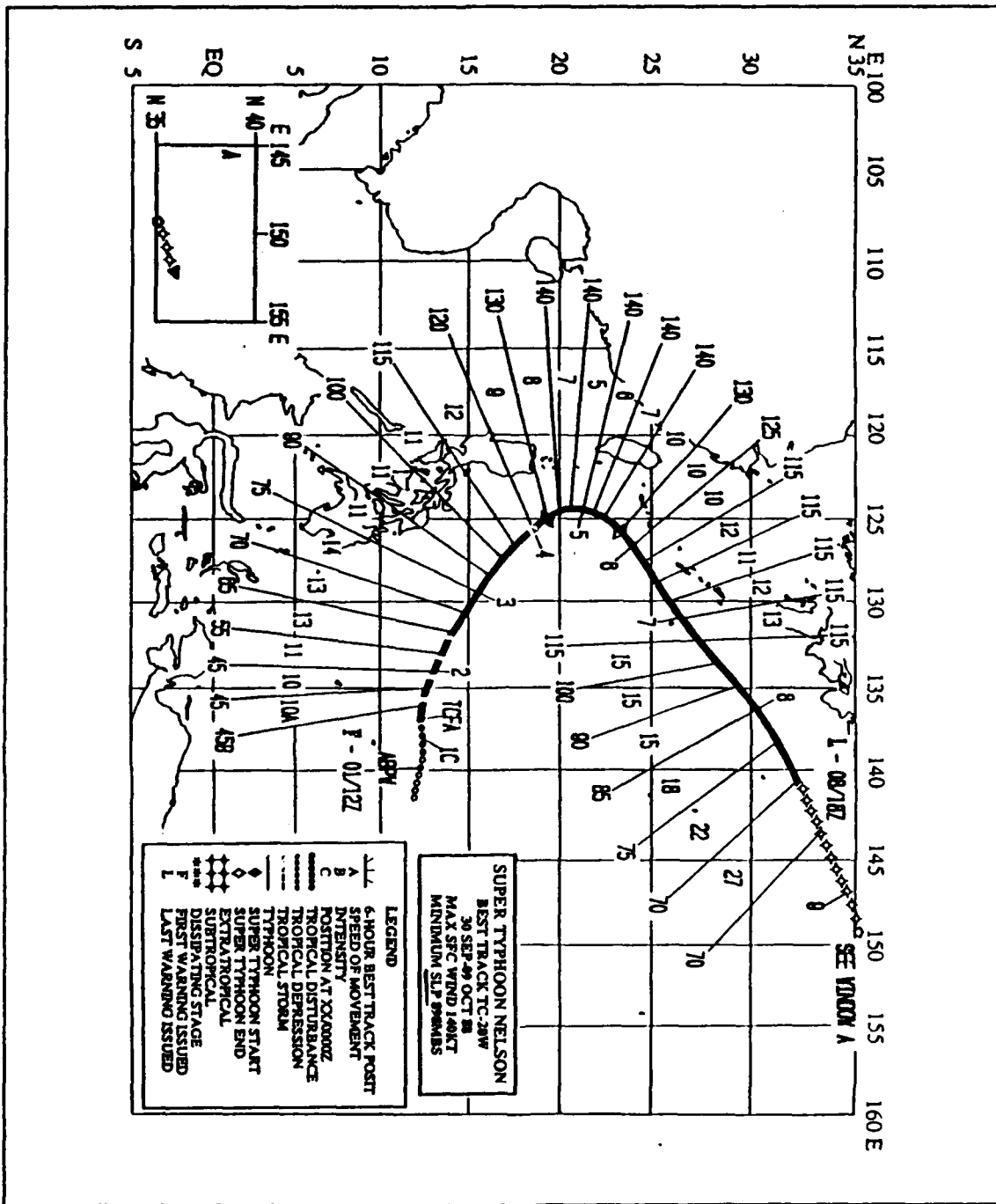
7

Figure 1.   Best Track positions of Typhoon Nelson from 30 Sept-9 Oct 1988 (ATCR 1988).

cyclone are not represented well due to the sparsity of observations. To overcome this limitation, NORAPS data with a resolution of 80 km will be used later to describe these features.

1. 0000 UTC 4 October 1988

The post-storm analysis (best track) has Typhoon Nelson located at 18.5°N, 125.8°E with winds of 120 kt. The storm track is to the northwest at a speed of 11-12 kt. Significant 300 mb features during this period (Fig. 2a) include a trough that extends from 31°N, 120°E to 24°N, 119°E. The position of the trough with respect to Nelson is advantageous in the rapid intensification or sustained development of the tropical cyclone. According to Elsberry (1987), the development of a strong outflow channel to the westerlies as an upper-level trough approaches or develops to the west of the cyclone is advantageous for system development. The outflow jet provides a good exhaust system for the storm and thus enhances intensification. A col area is located just west of Taiwan between two anticyclones: one positioned east of the storm at 21°N, 136.5°E, and the other located over southern China. The anticyclone east of the storm provides good outflow, so continued intensification is expected.

The midlevel analysis (Fig. 2b) is dominated by a high pressure center located at 23.5°N, 113°E and the subtropical ridge (STR) located over the western Pacific. The 500 mb flow indicates movement along the periphery of the STR. However, the movement and intensity of the high pressure cell over southern China is also a factor determining the direction in which Nelson will propagate. Typhoon Nelson appears to be moving toward the break in the ridge northwest of the storm postion, which is represented by a col area northeast of Taiwan.

2. 1200 UTC 4 October 1988

Typhoon Nelson is now located at 20°N, 124.7°E and has peak winds of 140 kt. Nelson is tracking through an area where a large number of tropical cyclones reach supertyphoon intensity, according to the 1970 Joint Typhoon Warning Center. Although the storm continues to track to the northwest, its speed of propagation has decreased to 7-8 kt.

A key 300 mb feature is the location of a weakness in the ridge line with respect to Nelson (Fig. 3a). This feature extends from 30°N, 121°E to 25°N, 121°E. The strong winds in excess of 50 kt to the northwest of the storm center provide a good outflow jet, which aids in the intensification of the tropical cyclone. The upper-level col located at 24°N, 121°E has propagated very slowly to the east. However, precise displacement of this feature is in doubt due to the sparsity of observations in this area.
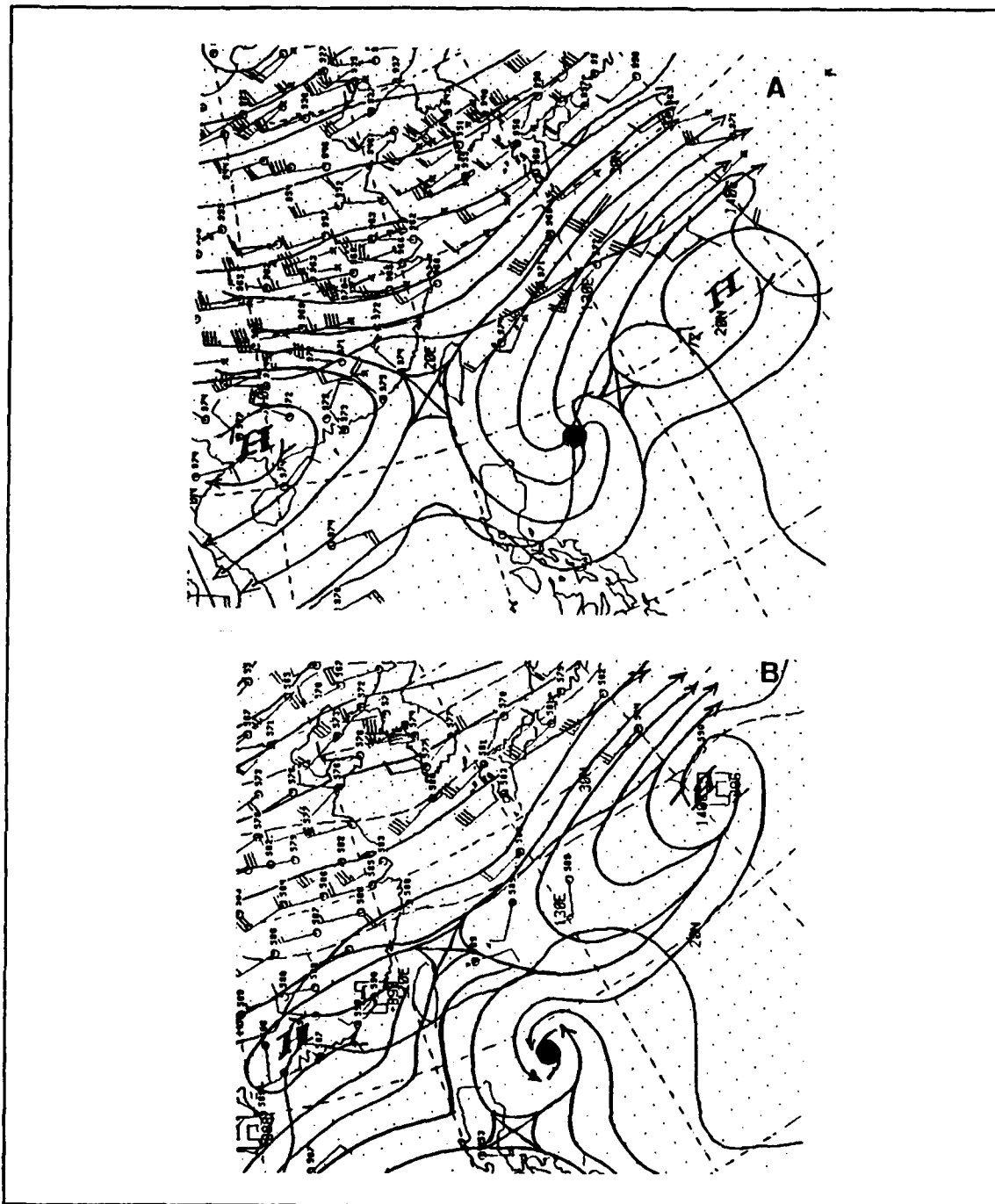
9

Figure 2.   NOGAPS analysis for 00 UTC 4 Oct 1988 at(A) 300 mb and (B) 500 mb.   Streamlines are analyzed in the region of Typhoon Nelson (dot) and the sub-tropical highs.

An analysis of the mid-level flow provides the reasoning for the slow propagation of Typhoon Nelson (Fig. 3b). Nelson continues to track around the periphery of the STR towards the area of least resistance. The storm is located in an area of weak mid-level winds just south of the col between the high cell located at 22°N, 111°E and the STR. The northeast-southwest orientation of the subtropical ridge axis contributes to more meridional steering flow.

3. 0000 UTC 5 October 1988

During this period, Typhoon Nelson has begun to recurve to the northeast. The storm is located at 21.3°N, 124.4°E with winds of 140 kt. The 300 mb circulation shows slight troughing to the northwest of the storm (Fig. 4a). Strong winds on the downstream side of the trough and on the periphery of the western Pacific ridge continue to be in the proper position to aid in the intensification of Nelson. The col located over Taiwan and the anticyclone located over southern China have remained relatively stationary in the last 12 h.

The movement of Nelson has slowed to 5 kt as recurvature is occurring. The 500 mb analysis shows that the high over southern China is building (Fig. 4b). The winds between the two highs in the region of the storm are opposing, which may be a factor in the slow propagation of Nelson. The col northeast of Taiwan has remained stationary as Nelson continues to track toward the area of least resistance.

4. 1200 UTC 5 October 1988

Typhoon Nelson is located at 22.5°N, 125.1°E with winds of 140 kt. Nelson is propagating to the northeast at 7-8 kt. The upper-level analysis shows a midlatitude trough located at 30°N, 115°E is approaching from the northwest (Fig. 5a). The strongest winds associated with the downstream side of the trough are located to the northwest of the storm center. This flow, in addition to the winds associated with the western Pacific ridge, still provide an excellent upper-level outflow. The col located over Taiwan has remained stationary in the last 12 h. Although the trough and Nelson are quite close, Nelson continues to be a warm core system with little or no penetration of cold air from the north.

Analysis of the mid-level features (Fig. 5b) shows a strong tendency for continued movement toward the northeast. The circulation pattern has not changed significantly in the last 12 h. The steering flow near the storm center is to the northeast along the periphery of the STR. The location of the col and the high over southern China are unchanged. The only significant change is a slight intensification of the STR,
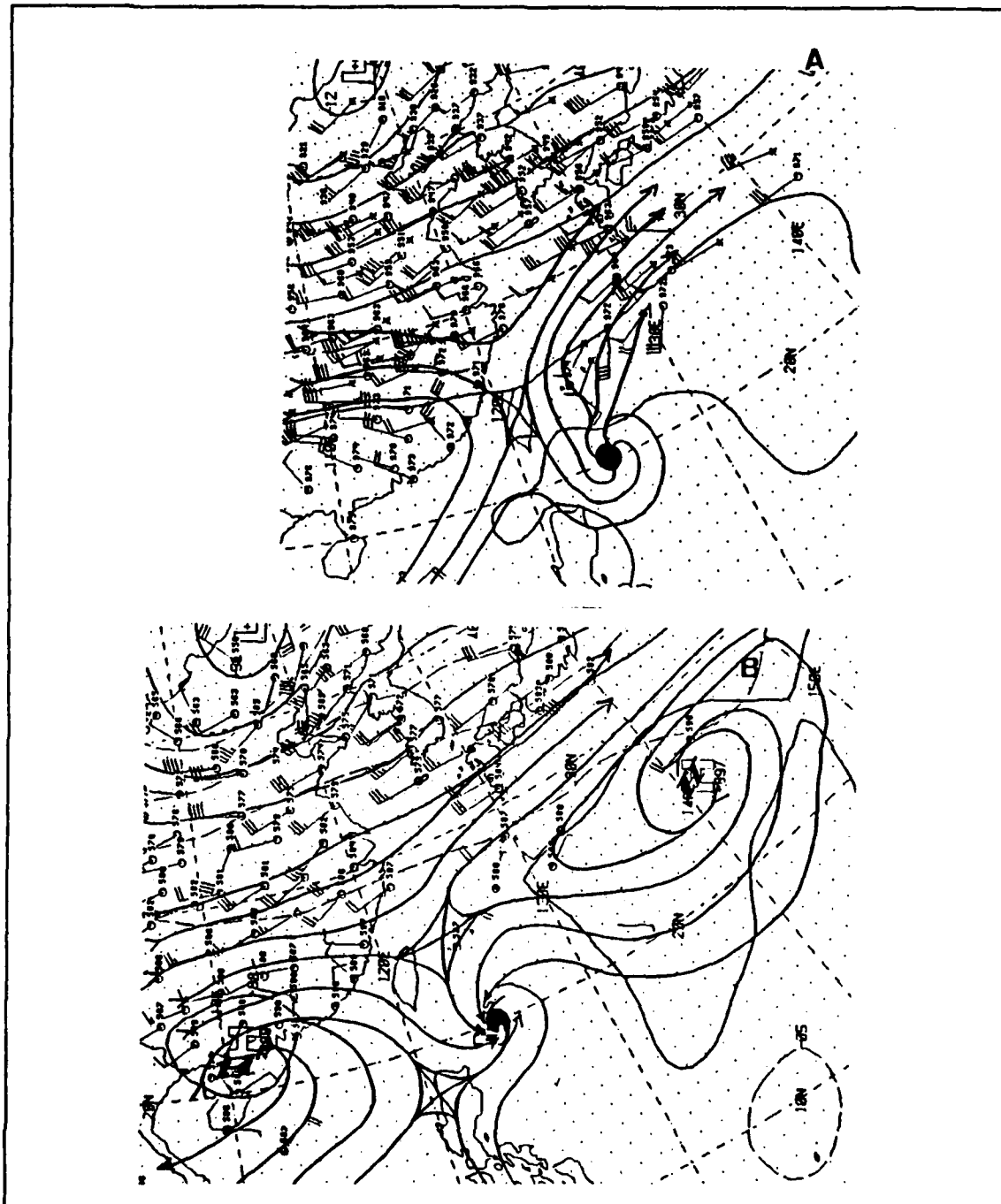
Figure 3.   As in Fig. 2, except for 12 UTC 4 Oct 1988.

although the analyzed change in intensity may be suspect due to the sparsity of observations in this region.
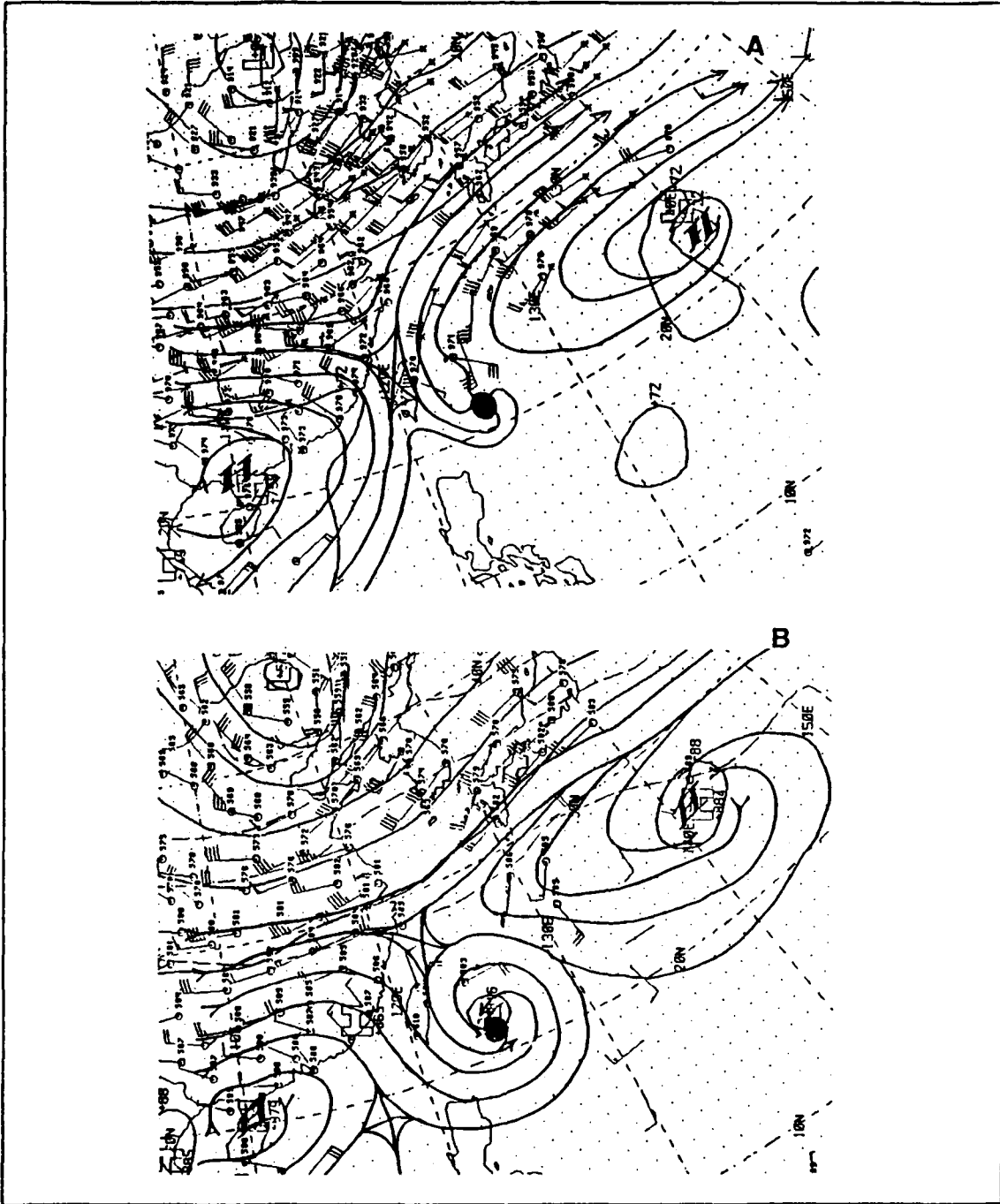
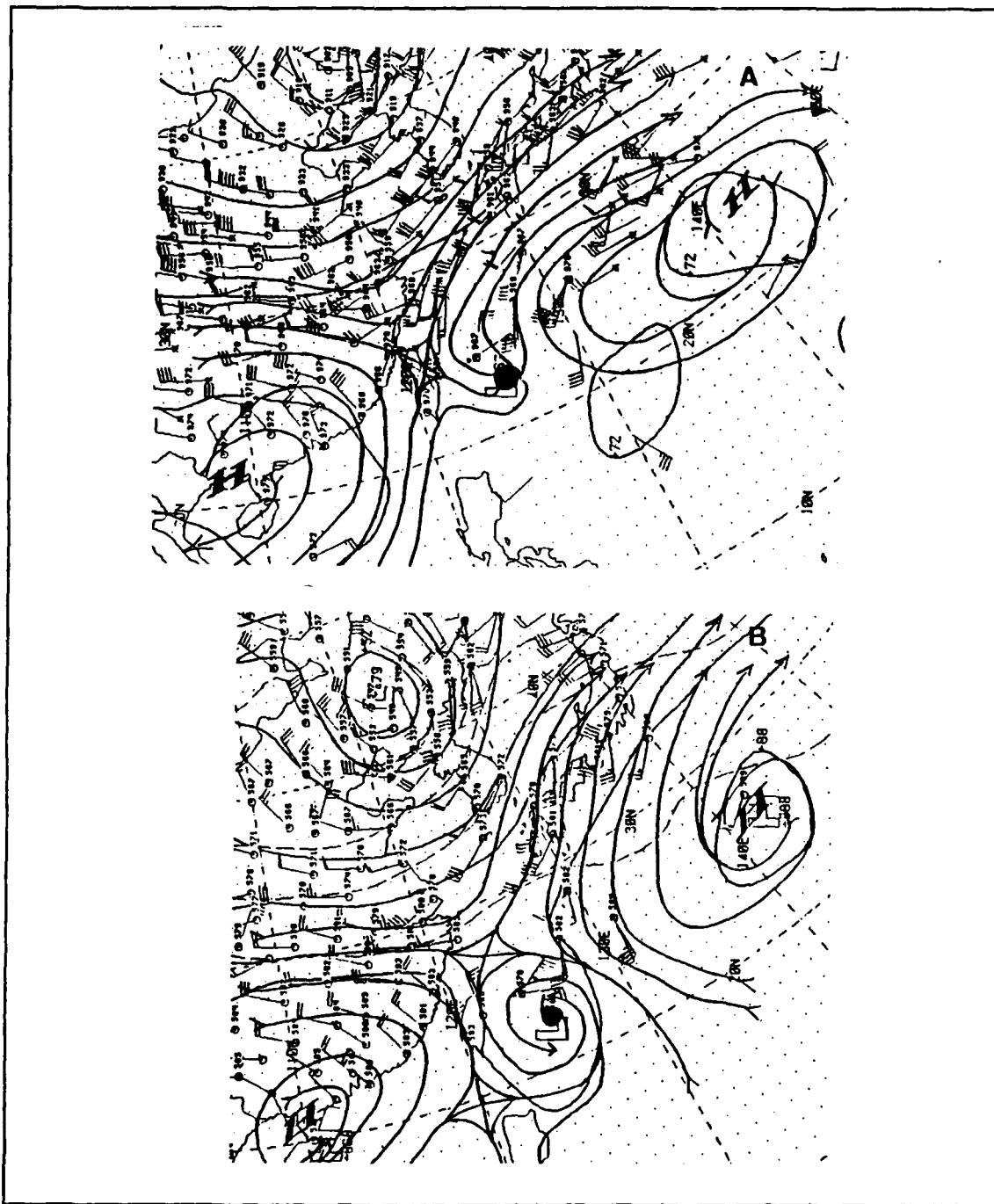Figure 4.   As in Fig. 2, except for 00 UTC 5 Oct 1988.

Figure 5.   As in Fig. 2, except for 12 UTC 5 Oct 1988.

5. 0000 UTC 6 October 1988

Typhoon Nelson has continued to track to the northeast at 10 kt, and it is now located at 24.0°N, 126.7°E and has weakened with peak winds of 125 kt. The upper-level analysis (Fig. 6a) shows cyclonic circulation has developed around Nelson. The col area now located at 27°N, 126°E has slowly drifted to the east and is located directly north of the storm. The trough has also propagated to the east as it extends from 32°N, 126°E to 27°N, 126.2°E. The trough remains west of the cyclone and is becoming more north-south aligned. Although the typhoon is getting closer to the midlatitude trough, the systems remain separate. The downstream side of the trough still provides a good outflow. However, the upper-level winds in this region have weakened in the last 12 h due to the orientation of the trough with respect to the position of the tropical cyclone. Nelson begins to lose the upper-level support that is so critical for storm development and maintenance.

The mid-level analysis (Fig. 6b) shows the midlatitude trough has deepened as it extends from 34°N, 131°E to 28°N, 128°E. The col area has propagated to the east and is located directly north of the cyclone. Strong (50 kt) winds from the north are converging into the western side of the storm. The typhoon begins to accelerate to the northeast as the steering flow around the periphery of the STR, which appears to have intensfied during the last 12 h. Again, analyses of intensification of this system are suspect due to the lack of observations. A significant aspect of this analysis is that the recurvature of Nelson is continuing due to the interaction with the midlatitude trough. even though the two systems remain distinct features separated by the col area.

6. 1200 UTC 6 October 1988

Nelson, located at 25.3°N, 128.9°E with winds of 115 kt, continues to weaken. move northeastward (at 12 kt) and accelerate. The most significant feature is that the tropical cyclone is clearly to the north of the ridge line connecting the two highs. This indicates that Nelson is definitely embedded in the westerlies. This feature is obvious in the 300 mb analysis and becomes apparent later in the 500 mb analysis. The upper-level col (Fig. 7a) between the tropical cyclone and the midlatitude trough continues to drift to the east. The downstream winds to the south of Japan still provide a good outflow, and Nelson maintains typhoon strength even as it propagates to the north over lower ocean temperatures.

The 500 mb analysis has Nelson embedded in the westerlies (Fig. 7b). Although the trough north of the storm seems to have weakened, the winds between the trough and Nelson remain strong.
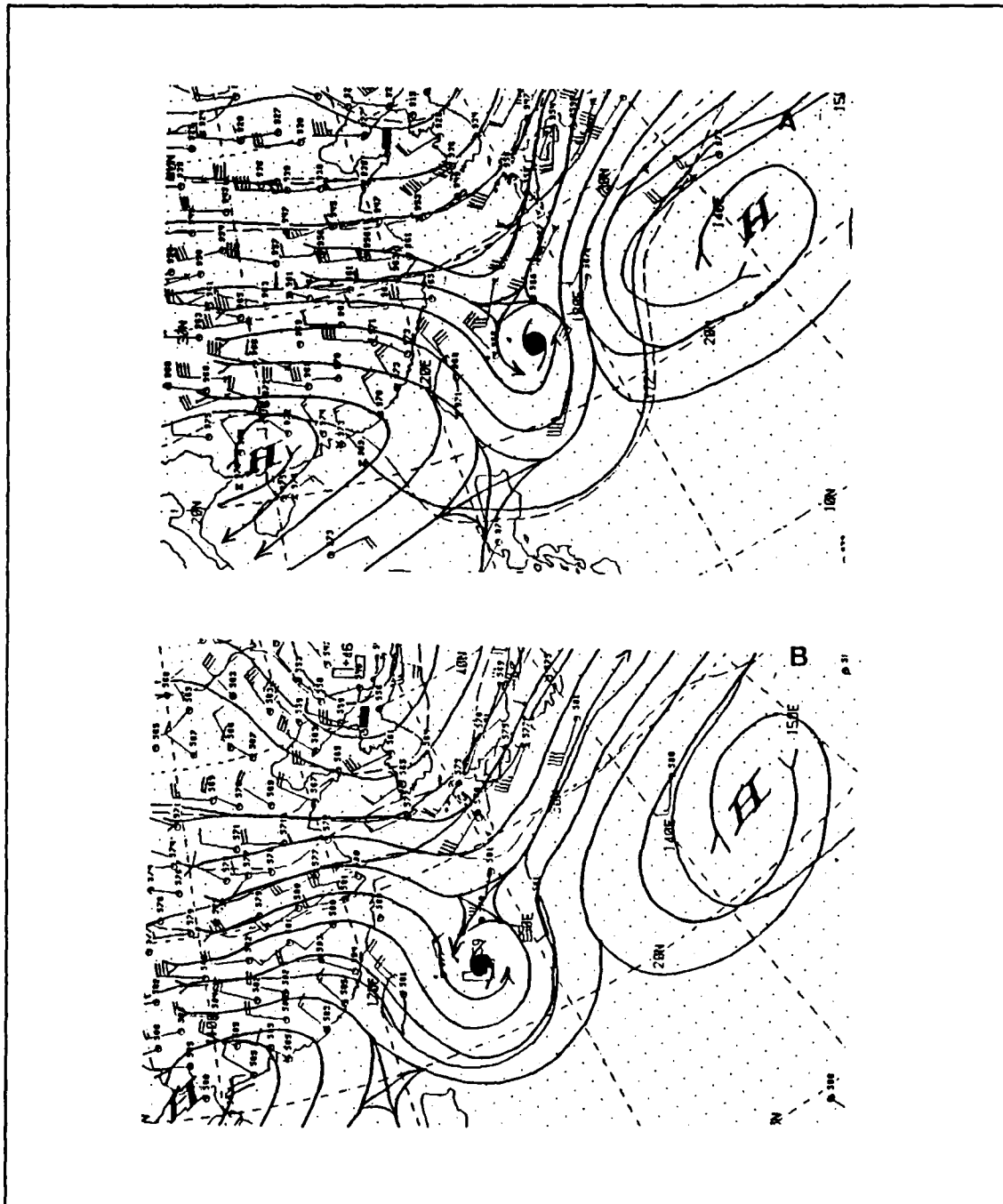
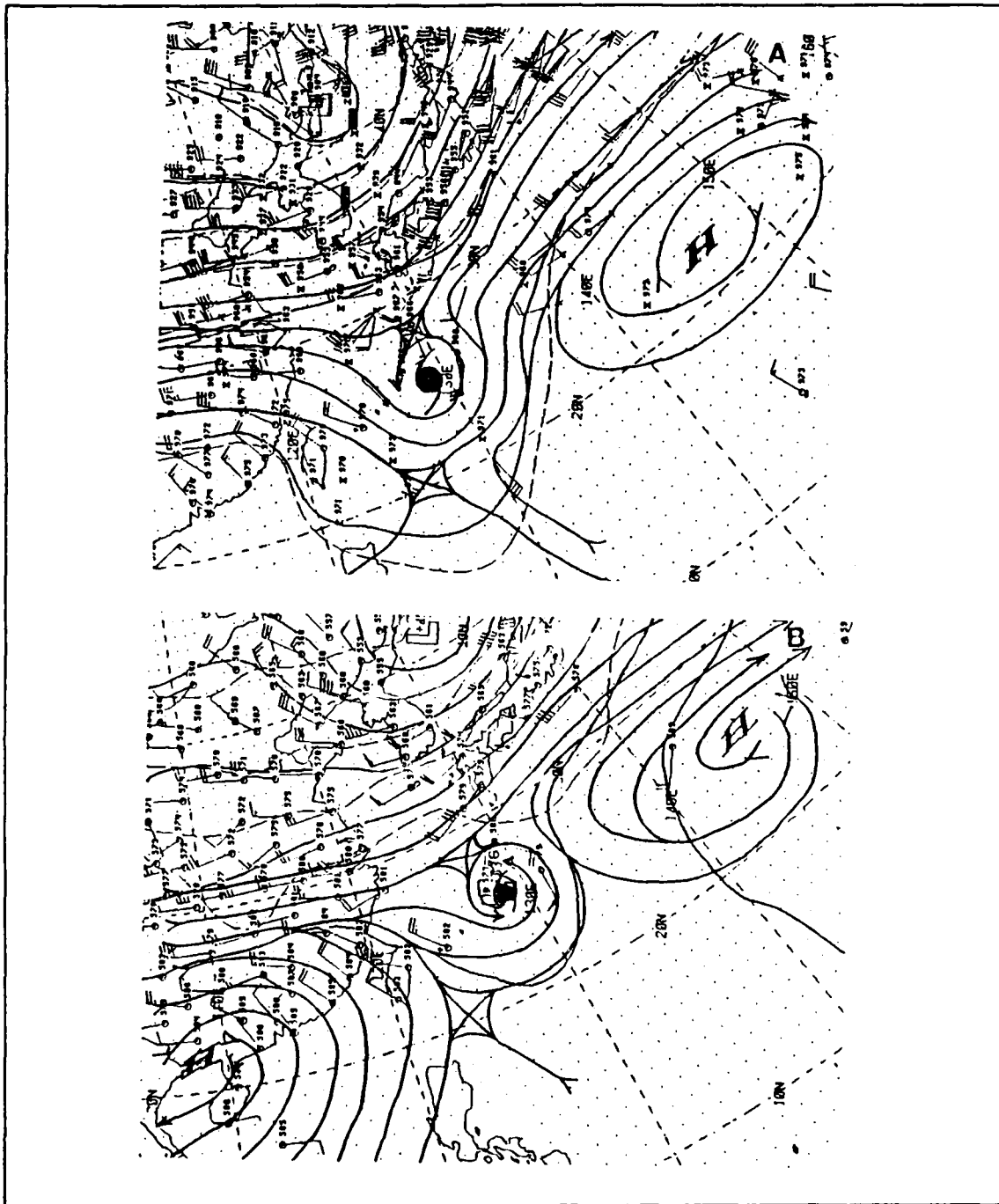Figure 6.   As in Fig. 2, except for 00 UTC 6 Oct 1988.

Figure 7. As in Fig. 2, except for 12 UTC 6 Oct 1988.

7. 7-8 October 1988 (Demise of Typhoon Nelson)

Nelson continues to weaken as it accelerates northeastward. The typhoon loses its tropical characteristics and transitions to an extratropical system southeast of Tokyo, Japan at 1500 UTC 8 October 1988. By this time, the storm was moving at a speed of 28 kt. Although it is becoming extratropical, Nelson maintains winds of typhoon intensity. The final warning on Nelson was issued on the 1800 UTC 8 October. Remnants of the storm were visible on satellite imagery for two days after the final warning.

Typhoon Nelson was the only supertyphoon of the 1988 typhoon season. Fortunately, the track to the west-northwest and subsequent recurvature to the northeast kept the storm away from populated areas and major damage was avoided.

As mentioned, it is extremely difficult to analyze the interaction of Typhoon Nelson with the extratropical cyclone using conventional synoptic data. Higher resolution data are required to accurately depict these small-scale features. NORAPS analyses and forecasts will be used to describe these features because the 80 km resolution should be sufficient in determining the interaction during recurvature of Nelson. Of course, analysis of model data is only reasonable if the model provides a good forecast of the storm evolution. Data, such as might be obtained during the tropical cyclone motion field experiment during 1990 (Abbey and Elsberry 1989), will be necessary to prove that the model description is valid.

B. FORECAST OF TYPHOON NELSON

If the NORAPS fields are to be used to infer the IPV interactions during recurvature, it is essential that the NORAPS accurately predict the movement of Typhoon Nelson. According to Hodur (1988), NORAPS demonstrated skill in predicting the path of storms during the 1988 typhoon season, especially for storms poleward of 20°N. For those storms equatorward of 20°N, NORAPS had a rightward bias. Hodur (1988) states the major reason for tropical cyclone forecast failures in NORAPS during 1988 was due to the inability of the model to handle moisture and its interaction with radiation. However, Typhoon Nelson was selected for this study because it did interact with a midlatitude trough and because NORAPS did a reasonably good job in forecasting the recurvature to the northeast.

The forecasters at JTWC use various tools in forecasting tropical cyclone movement: Climatology (CLIM), Half Persistence and Climatology (HPAC), two analog programs (RECR and TOTL), the One-Way Tropical Cyclone Model (OTCM), Extrapolation (XTRP) and Climatology and Persistence (CLIPER). A discussion of these

18

aids can be found in the ATCR, 1988. The various forecast tracks for Typhoon Nelson are shown in Fig. 8. Best track positions from 1200 UTC 1 October until 0000 UTC 4 October, and the subsequent forecast positions at 24, 48 and 72 h, are shown.

The majority of the forecast schemes accurately forecast the recurvature of Nelson. The largest differences among the schemes are related to how fast and how far west Nelson would propagate. The JTWC and NORAPS forecasts have Nelson farther to the east than the other schemes, especially at 72 h. The center of the storm in the NORAPS forecast was assumed to be at the center of the maximum in the IPV fields presented in the next section.

The post-storm analysis (best track) at 1200 UTC 4 October 1988 had Typhoon Nelson located at 18.5°N, 124.7°E, whereas NORAPS had the storm located at 20.3°N, 126.1°E. This 200 km error to the east indicates that the model recurved the storm too soon. By 0000 UTC 5 October 1988 Nelson began to recurve to the northeast and was located at 21.3°N, 124.4°E. The NORAPS forecast position was at 21.3°N, 126.4°E. Although the storm actually remained relatively stationary in the last 12 h, the NORAPS forecast has the storm far to the east because of the early recurvature. Nelson has begun its propagation to the northeast as indicated by the 1200 UTC 5 October 1988 position at 22.5°N, 125.1°E. Although NORAPS accurately predicted a track to the northeast, the forecast position of 23.1°N, 126.5°E still shows an eastward bias. Nelson continues to move to the northeast and at 0000 UTC 6 October 1988 it is located at 24.0°N, 126.7°E. The 48-h NORAPS forecast has Nelson positioned at 24.5°N, 127.7°E. Although there is still an eastern bias in the model forecast, the position error is only 148 km. At 1200 UTC 6 October 1988 Nelson is located at 25.3°N, 128.9°E and the NORAPS position is at 26.8°N, 128.9°E. Although the easterly bias in the previous forecast periods has been eliminated, the model has continued to accelerate the storm farther to the north. For the final forecast period (ending at 0000 UTC 7 October 1988), Nelson is located at 26.6°N, 131.1°E, whereas the NORAPS position is at 29.6°N, 133.6°E. The model has pushed the storm too far to the northeast with a 72-h error of 388 km.

Overall, NORAPS did an excellent job in forecasting the movement of Typhoon Nelson. As mentioned above, the relatively stationary position of the large-scale features that control the typhoon movement probably contributes to the accurate forecast.
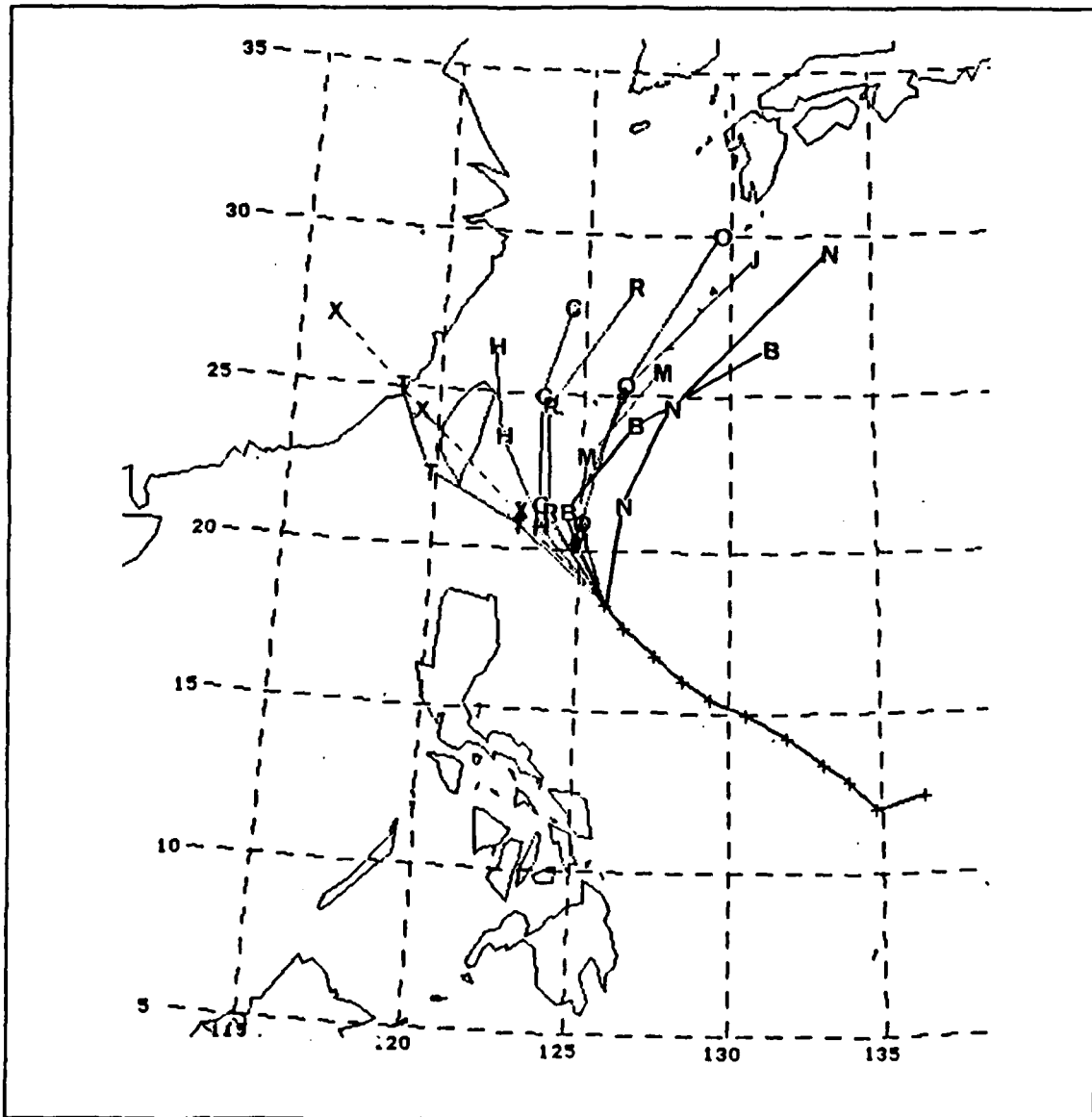
19

Figure 8. Tracks of Typhoon Nelson forecast by various aids where XTRP(X), TOTL(T), HPAC(H), CLIPPER(C), RECR(R), OTCM(O), JTWC(J), CLIM(M), NORAPS(N) and Best Track(B). The letters along each track indicate the positions at 24, 48 and 72 h after the initial time of 0000 UTC 4 Oct 1988. Earlier storm positions with a 12-h interval are indicated by +.

20

IV. DESCRIPTION OF TYPHOON NELSON IN TERMS OF IPV.

The synoptic analysis of Typhoon Nelson using NOGAPS 300 and 500 mb height fields indicates that the interaction between the midlatitude and tropical cyclones occurs on horizontal scales that are too small to be accurately represented by synoptic-scale data. The major problem is the deficiency in horizontal and vertical resolution due to the lack of observations in the vicinity of the tropical cyclone. By using model fields with 80 km horizontal resolution and 21 level vertical resolution, these "gaps" in data are filled with dynamically consistent model data. The analysis of isentropic potential vorticity (IPV) fields in Typhoon Nelson illustrates two interesting features. First, the vertical and horizontal structure of the bogus vortex is analyzed to determine the effect it may have on the NORAPS forecast. Second, the IPV advection pattern associated with the storm center and other synoptic features are examined in relation to storm propagation.

A. HORIZONTAL AND VERTICAL STRUCTURE OF THE BOGUS STORM

Hodur (1988) states that the bogus vortex used in NORAPS is much larger than typical tropical cyclones and this may degrade the track forecast, especially in low latitude forecasts. The large radial extent of the bogus storm is seen in the horizontal representation of Typhoon Nelson in terms of IPV (Fig. 9a). The center of Typhoon Nelson at 310 K corresponds to the maximum value of IPV because the relative vorticity is a maximum inside the radius of maximum winds. Large values of IPV encircle the storm center, with highest values to the extreme east and west of the storm. The radial width of the IPV associated with the storm is surprisingly broad for the low levels of a tropical cyclone. Moreover, the horizontal scale of the cyclonic winds also appears to be unrealistically large as the bogus vortex dominates the western North Pacific area.

The bogus storm is clearly depicted on the 320 K surface (Fig. 9b). Although isolines of IPV still encircle the storm center, the vortex is not circularly symmetric at larger radii because a larger node of IPV extends southward and a maximum of $3.5 \times 10^6 mKs^{-3}mb^{-1}$ is found just north of Taiwan. Another secondary maximum is found in the southwest corner. The large gap between the tropical storm and the maximum IPV associated with midlatitude systems also is evident.

The upper-tropospheric IPV representation of the initial bogus storm is shown in Fig. 10a. Maximum IPV values are found at the 340 K level. A strong westerly jet is
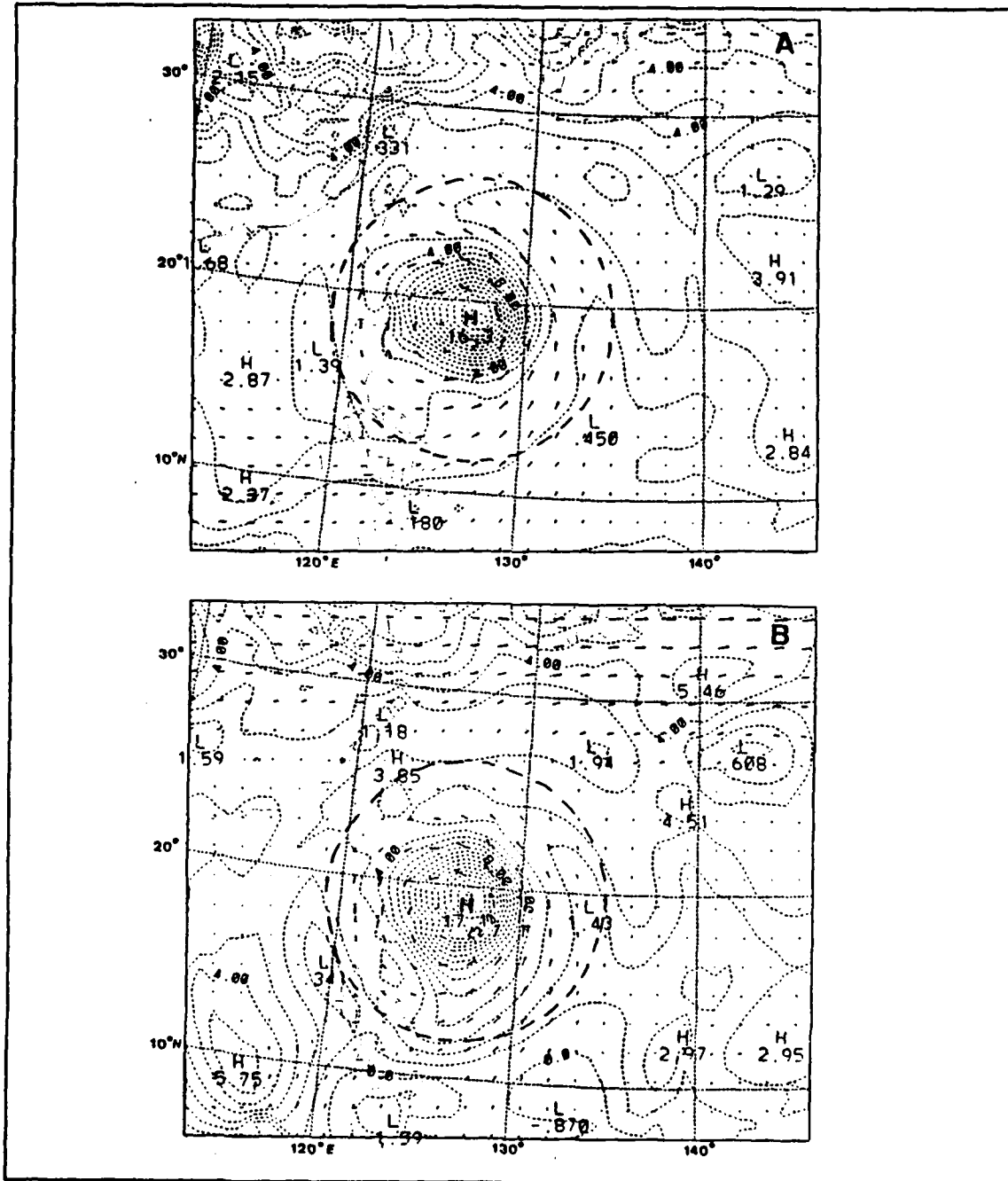
21

Figure 9.   IPV at 0000 UTC 4 Oct 1988 on (A) 310 K and (B) 320 K surfaces. Wind speeds are proportional to the length of the vectors and IPV contours are $1 \times 10^6 mKs^{-3}mb^{-1}$. Heavy dashed line is the 800 km radius.

22

depicted along the northern boundary with a IPV dipole of high (low) values on the cyclonic (anticyclonic) side to the northeast of the storm center. A ring of low IPV values encircles the storm and the values are actually negative to the west and southwest of the vortex. These minima are on the boundary between cyclonic flow in the storm and the anticyclonic outflow. An IPV maximum is found northwest of the vortex where the anticyclonic flow on the edge of the vortex interacts with the westerly wind maximum to the north. This feature is also found higher in the troposphere on the 350 K surface (Fig. 10b). In the 350 K surface, another maximum of IPV larger than the bogus vortex is located just west-northwest of the vortex center. The values of IPV near the center of the vortex are smaller then at the 340 K surface as the cyclonic flow around the center is not as strong. However, large negative values of IPV are found to the south of of the vortex center along the edge of a band of strong easterly flow. In summary, this upper-level IPV representation of the tropical cyclone and the midlatitude flow would seem to indicate a strong interaction is already occurring with southerly and southwesterly flow to the northwest of Nelson.

The vertical structure of these features relative to the vertical structure of the bogus vortex is indicated by a vertical cross-section from 29°N, 119°E to 12°N, 132°E in Fig. 11a. The lower boundary corresponds to the 300 K surface and the upper boundary is along the 350 K surface. Limiting the upper boundary to 350 K removes the extremely large IPV values associated with the stratospheric stratification. These stratospheric features are not considered relevant for this study. Cyclonic flow around the vortex is represented as positive negative wind values to the right/left of the storm center, which is represented by the zero isoline. The warm core structure of the bogus vortex is indicated by the downward depression of the 350 K surface over the vortex center.

In Fig. 11a the upper-tropospheric IPV maximum described above is located to the left (northwest) of the vortex. This feature extends into the lower troposphere with a secondary maximum at approximately 750 mb. A narrow region of negative IPV values extends downward to about 400 mb between the IPV maximum to the northwest and the maximum associated with the tropical cyclone. This negative IPV region is on the anticyclonic shear side of the zero isoline in the upper tropospheric outflow region. Another region of negative values of IPV located southwest of the vortex is illustrated by the cross-section in Fig. 11b. An interesting feature in both cross-sections is the vertical coupling of the upper and lower vortex structures. In both displays, the zero velocity isoline shows very little horizontal displacement. The large radial size of the

Figure 10. As in Fig. 9, except for (A) 340 K and (B) 350 K.
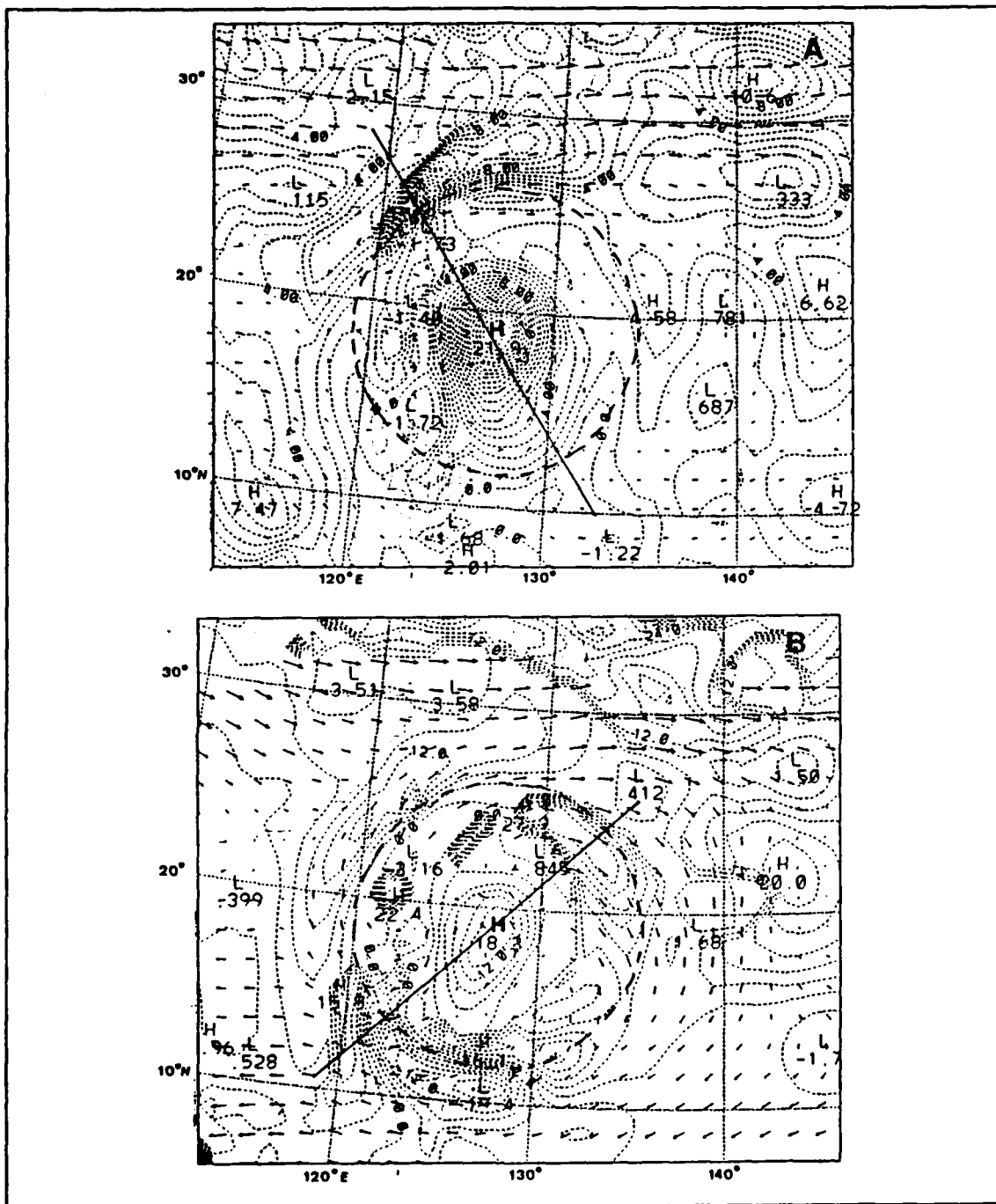
bogus vortex is also evident in the cross-sections as the positive IPV values around the vortex are extremely broad. This is another indication that the bogus vortex is too large (Hodur 1988, 1989).

After a 12 h integration, the large radial extent of the bogus vortex is still apparent (Fig. 12a). The bogus vortex has become more asymmetric as a lobe of low IPV has developed just southwest of the center. The cyclonic circulation is still extensive with a good inflow from the southwest. At 320 K (Fig. 12b), the vortex has become more compact. However, the circulation around the storm also includes asymmetries. These asymmetries may be due to adjustment in the model to compensate for the large warm core system represented by the bogus vortex. In the upper troposphere (Fig. 13a), the IPV field around the vortex has become extremely compact and oval in shape. The IPV field is oriented to north-south and with a significant wavenumber 2 component. This is a change from the initial conditions when the wind field was more circular. Negative values of IPV are located to the southwest and southeast of the storm center. An area with a large IPV maximum is found to the northeast of the storm center. These values are also evident in Fig. 13b. At this level, the cyclonic flow around the vortex has diminished.

An interesting feature that occurs after 12 h is the vertical displacement of the maximum value of IPV associated with the vortex center. In the initial bogus, the lower-level and upper-level features were well coupled. After a 12 h integration, the IPV maxima are not vertically stacked (compare Fig. 12b to Fig. 13a). The displacement to the south of the maximum value at upper levels is readily apparent in Fig. 14a. A "wobble" has been introduced into the vortex structure. This uncoupling of the upper and lower level may be due to the inability of the model to sustain the bogus vortex. The presence of negative IPV on the periphery of the bogus vortex may have led to inertial instability (Ciesielski et al. 1989), which displaces high values of PV along the periphery of the vortex. This unstable "wobble" is also seen in Fig. 14b as the low-level PV maximum is to the southeast of the upper-level maximum. Another interesting feature in both cross-sections is the difference of the maximum winds on the eastern side of the vortex as compared to those on the western side. Since this difference in velocity is due to the superposition of a vortex on the advecting flow, it should indicate propagation to the north.

Clear indications of stability in the bogus vortex occur after 36 h (Fig. 15a). To accommodate the movement of the storm, the grid has been displaced to the north. The most noticeable feature is the reduction in the size of the vortex compared to earlier
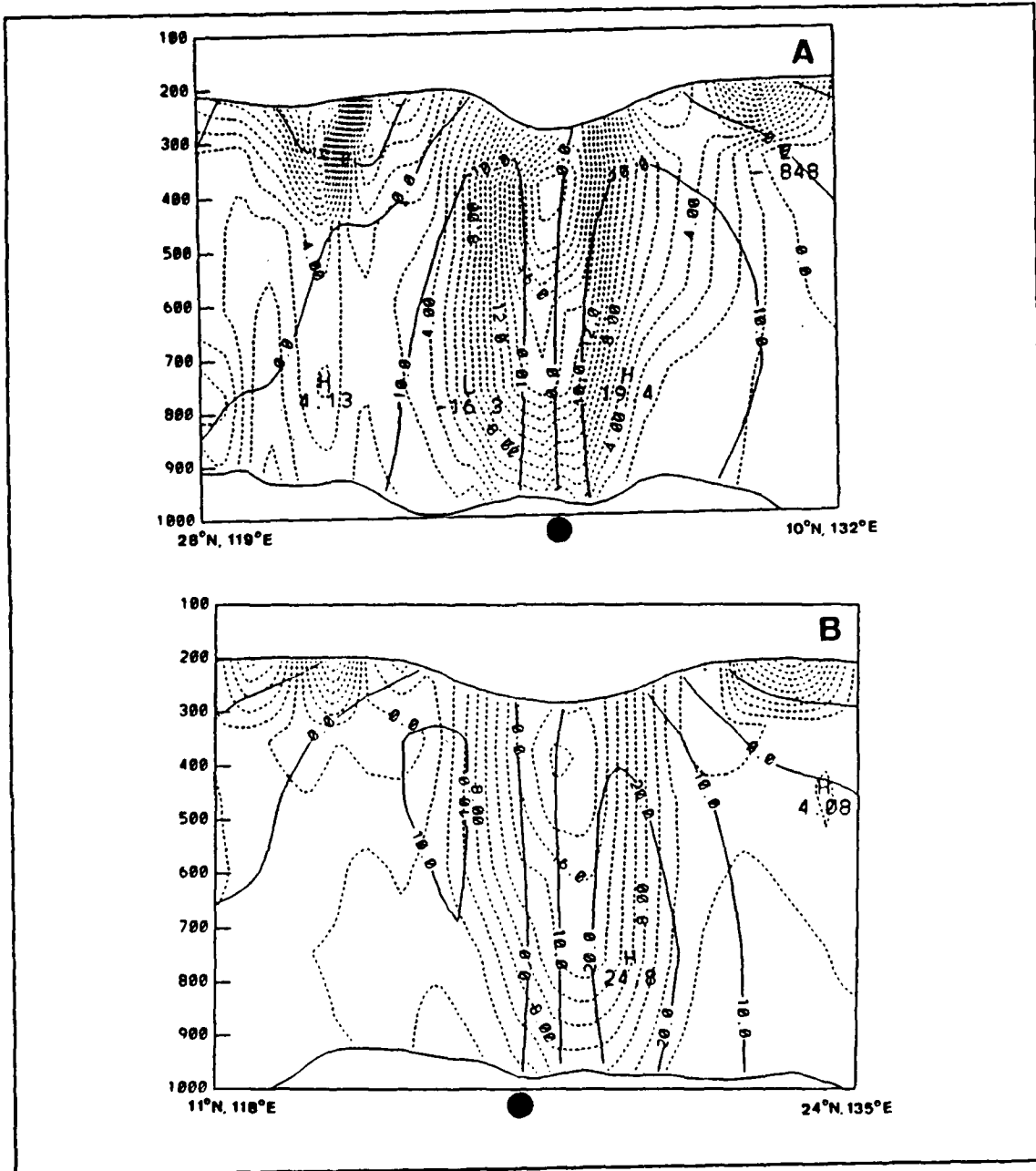
Figure 11.   Cross-section on 00 UTC 4 Oct 1988 from (A) northwest to southeast and (B) southwest to northeast.   Potential vorticity ($10^6 mKs^{-3}mb^{-1}$, dashed) and tangential wind components (m/s, solid) are shown between 300 K (lower boundary) and 350 K (upper boundary).   Orientation of cross-sections shown in Fig. 10.

Figure 13.   As in Fig. 10, except for 12 UTC 4 Oct 1988 at (A) 340 K and (B) 350 K.

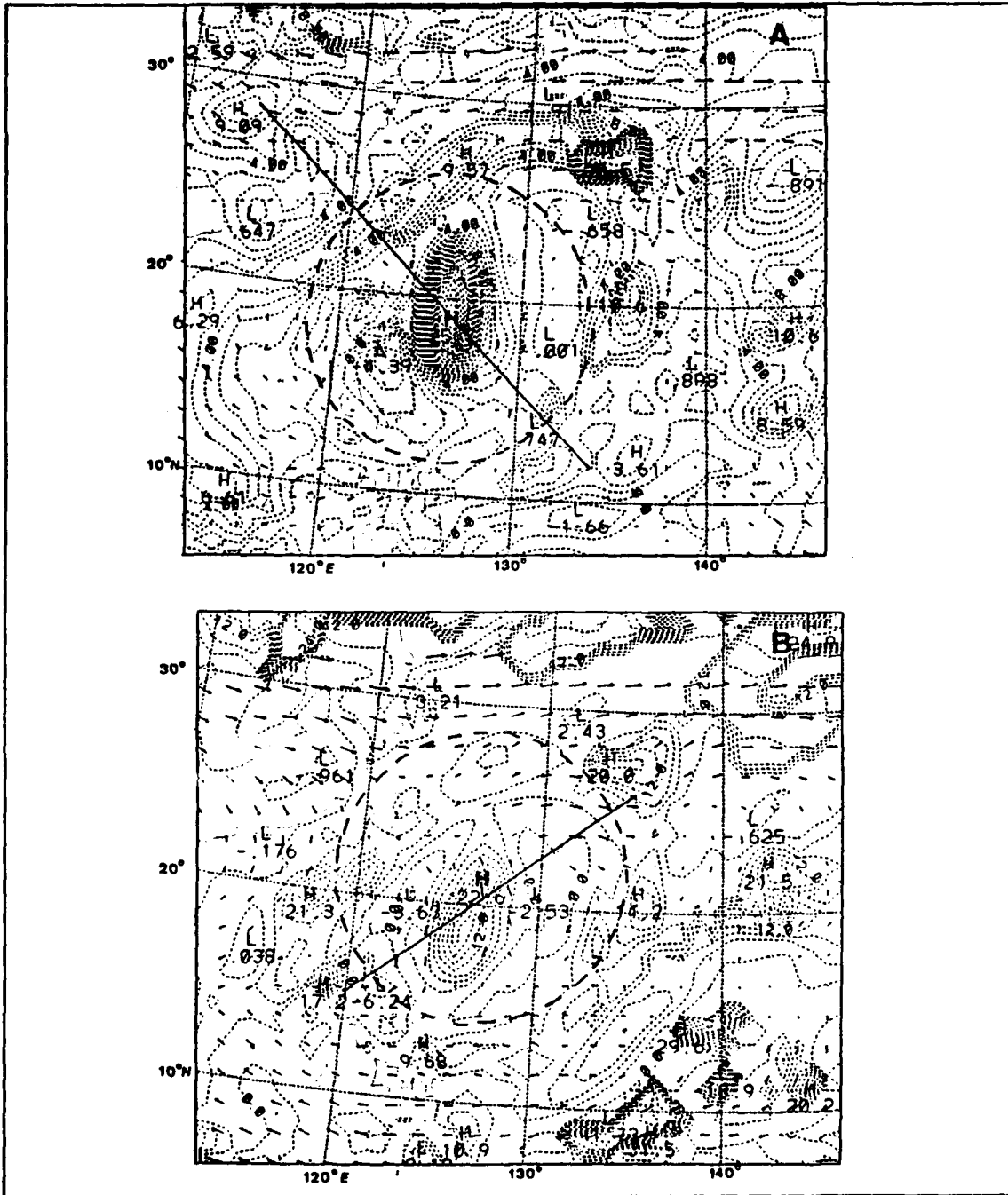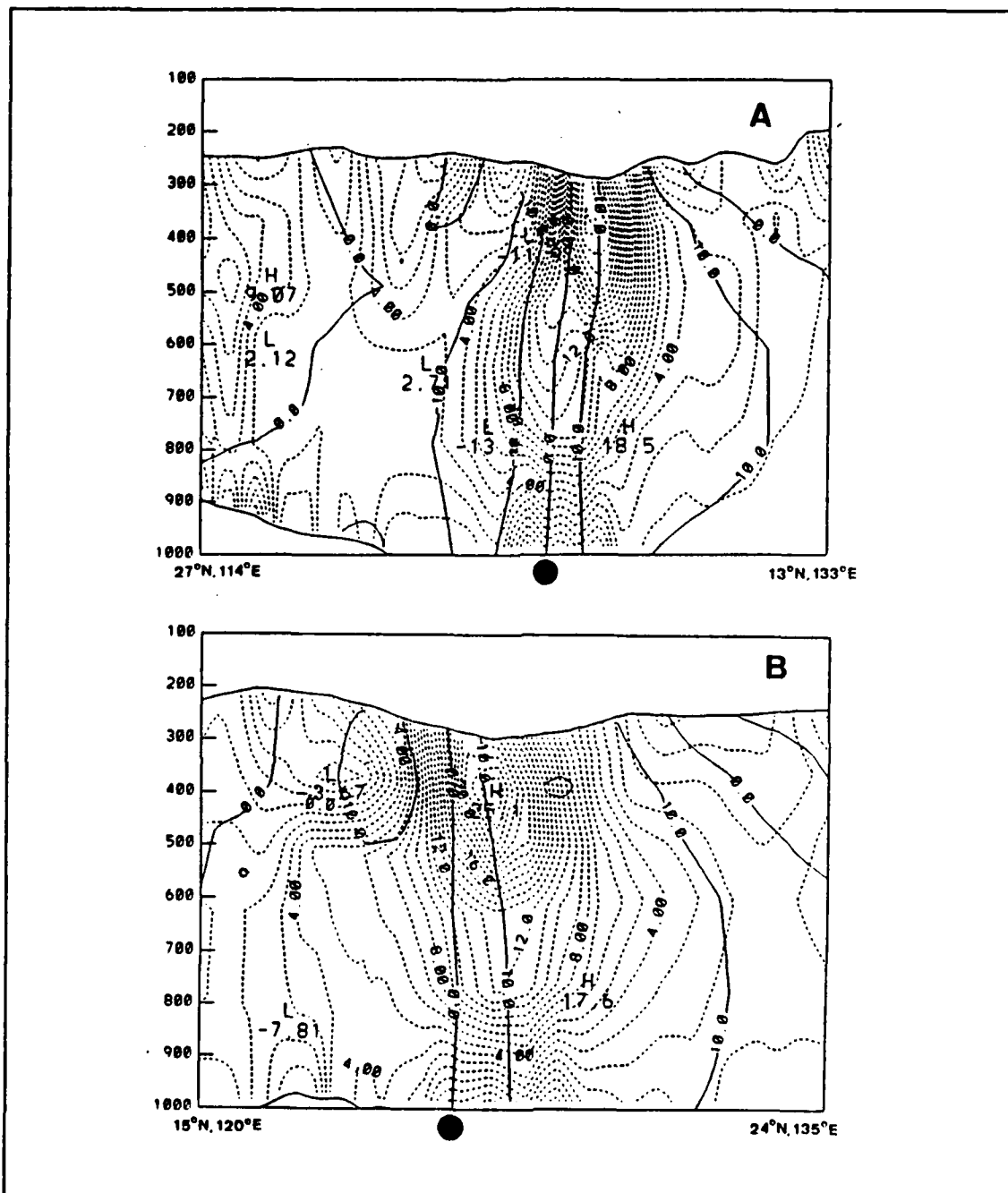Figure 14.   As in Fig. 11, except for 12 UTC 4 Oct 1988 for (A) northwest to the southeast and (B) southwest to the northeast.

times. The IPV maximum near the vortex center is more compact, and lobes of high IPV around the periphery of the vortex are not as numerous. However, the maximum

29

value of PV associated with the vortex center has almost doubled in 36 h. The model evidently has adjusted to the dynamical processes associated with the tropical cyclone and the IPV maximum now depicts the intense diabatic heating found near the storm center in the model.

High values of IPV along the periphery of the vortex are still apparent after 36 h in Fig. 15b, which may indicate that the model is still trying to adjust to the initial wind and mass fields. Although the IPV maximum at this level has also increased, the vortex is not as symmetric. The lobes of high IPV to the east of the vortex may be associated with the greater diabatic heating due to the advection of warm moist air from the southwest quadrant.

In the upper troposphere, the vortex circulation after 36 h is very compact (Fig. 16a). Small negative values of IPV are found in the anticyclonic cell to the east of the center. This feature is further enhanced at 350 K (Fig. 16b) as negative values of IPV are found to the east and west of the vortex. The lobe of cyclonic IPV to the northwest of the vortex represents an approaching midlatitude wave. The vertical extent of this feature is evident in Fig. 17a. The maximum of IPV associated with this short-wave extends downward into the midtroposphere to approximately 480 mb. This cross-section also illustrates that the vortex has become much more compact after 36 h. The lower-level and upper-level maxima of IPV are much better coupled. The stable structure of the vortex is also apparent in Fig. 17b, which again has very little vertical tilt. Since the "wobble" in the vortex has diminished, the model has adjusted the mass and wind fields to the diabatic heating associated with the vortex. If this structure better represents the "model dynamics" of the tropical cyclone, the bogus vortex that is inserted into the initial fields should resemble this structure rather than the broad vortex at 0000 UTC 4 October.

B. ADVECTION OF IPV FIELDS

Forecasters at the Joint Typhoon Warning Center (JTWC) make use of various objective aids to guide them in the forecast of tropical cyclones. Since only the track forecast and not the predicted fields are transmitted to JTWC, the forecaster has little opportunity to assess the dynamics involved in the model forecast. Without dynamical reasoning, the likely accuracy of the model forecast is difficult to assess. If the JTWC forecaster knew what dynamical features contributed to the track forecast, he/she would be able to assess the synoptic realism and monitor the relevant synoptic features during the course of the forecast.

30

Figure 15.   As in Fig. 9, except for 12 UTC 5 Oct 1988 at (A) 310 K and (B) 320 K.

Figure 16.   As in Fig. 10, except for 12 UTC 5 Oct 1988 at (A) 340 K and (B) 350 K.
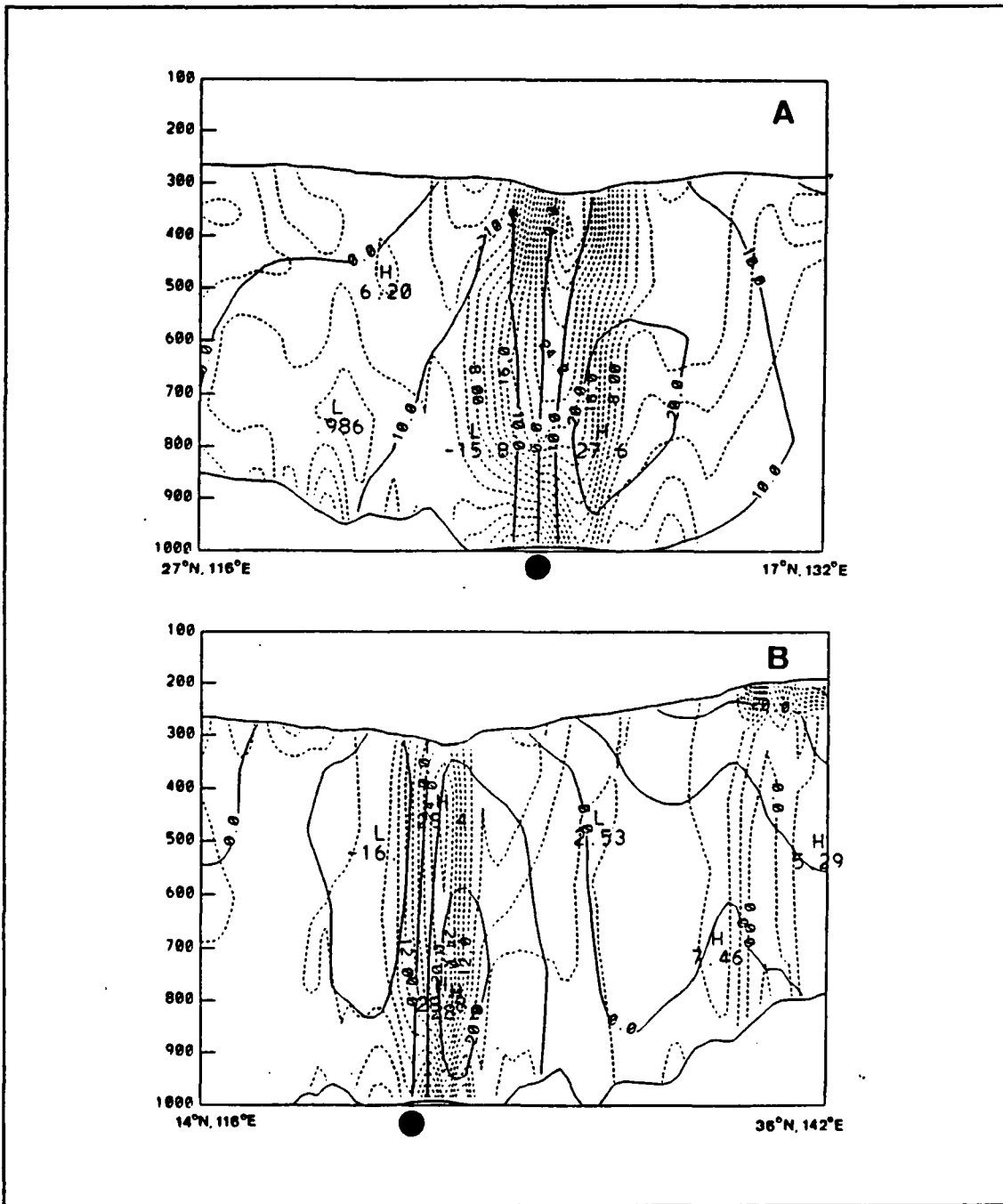
Figure 17.   As in Fig. 11, except for 12 UTC 5 Oct for (A) northwest to southeast and (B) southwest to northeast.

The purpose of this section is to illustrate the usefulness of a IPV advection field representation, and specifically how this may aid a forecaster in determining the contributions to storm movement due to self-advection, advection due to basic flow and the advection resulting from adjacent synoptic features. Two theta surfaces (310 K and 320 K) are selected to represent the mid-tropospheric steering flow. The two upper-level surfaces (340 K and 350 K) are presented for the initial period and after 12 h to show the effect of the bogus vortex on the IPV advection fields. The IPV advection fields are just one of the output fields generated by NORAPS that may be useful to the JTWC forecaster.

At 0000 UTC 4 October 1988, a large region of positive IPV advection (IPVA) is located to the northwest of the storm center (Fig. 18a). The positive/negative IPVA dipole associated with the flow around the vortex is the dominating feature at this time. A vector from the negative IPVA center to the positive IPVA center indicates the instantaneous IPVA tendencies, and suggests a northwestward track. Since no other significant IPVA centers are found near the vortex, it is expected that this motion tendency will continue for some time. A similar lobe configuration is found at 320 K (Fig. 18b), except both lobes are now asymmetric with a northeast-southwest elongation. However, the orientation of the IPVA centers with respect to the vortex still indicates movement to the northwest. As in the preceding figure, the advection pattern associated with the vortex is the dominant feature.

Maxima of IPV advection that are not associated with the storm center are found in the upper troposphere (Fig. 19a). Lobes of positive and negative IPVA are located northwest of the storm center. Although these lobes might appear to represent a mid-latitude wave, they are actually a result of the extremely broad bogus vortex. The advection pattern near the center is asymmetric as both lobes are elongated to the southwest. Connecting the maximum values of negative and positive IPVA again implies movement to the northwest. The effect of the over-sized bogus is also apparent in Fig. 19b. Maxima and minima values of IPVA are located along the outer periphery of the bogus vortex. Thus, the bogus vortex distorts the IPVA fields, which may lead to an inaccurate representation of the motion processes at this level.

After a 12 h integration, little change occurs in the lower tropospheric advection pattern (Fig. 20a). The positive (negative) IPVA center is still to the northwest (southeast) of the vortex center. The IPV advection pattern associated with the vortex remains the dominant feature. At 320 K (Fig. 20b), the advection patterns near the vortex have become more distorted. The negative lobe is extended farther to the south

34
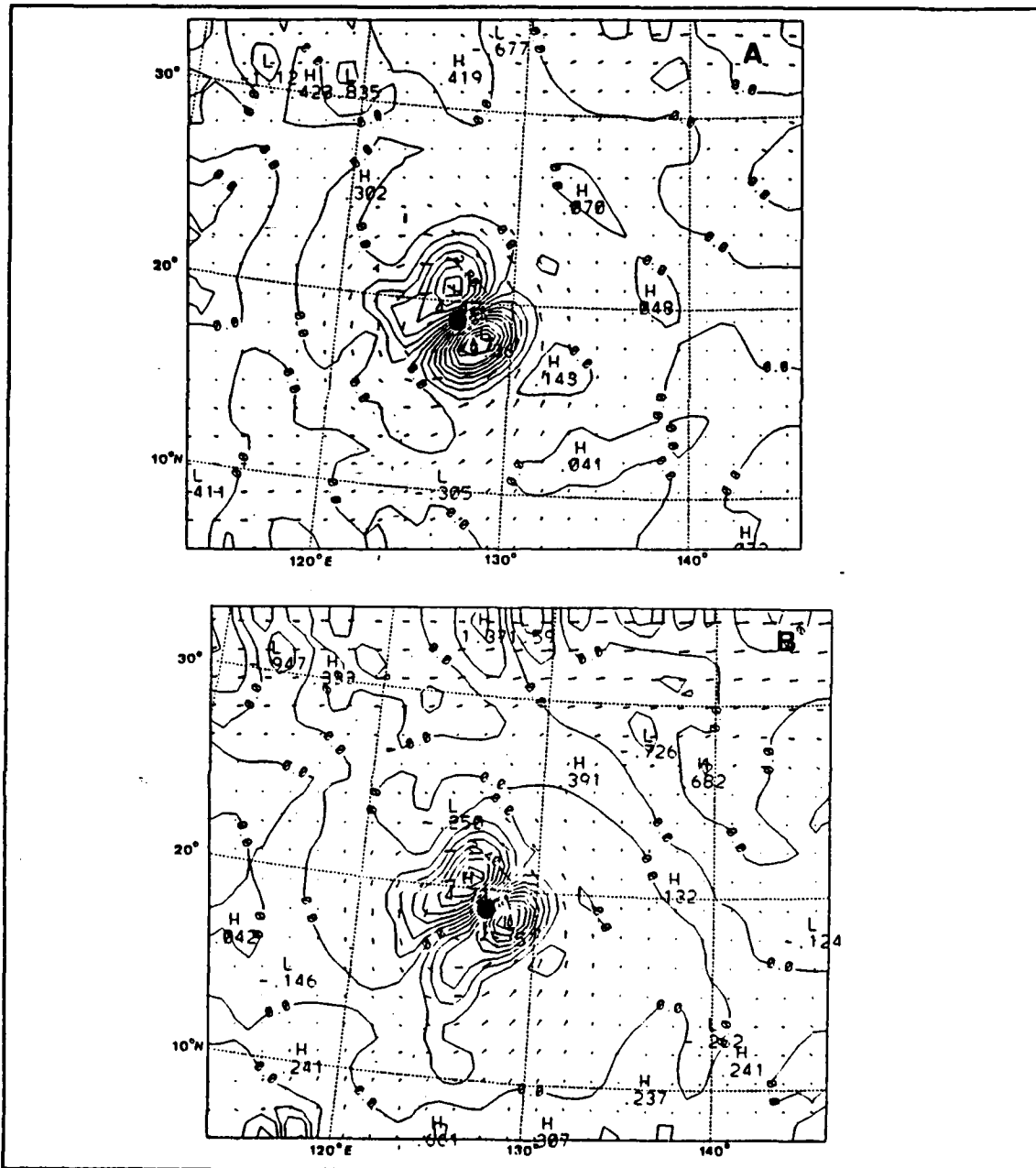
Figure 18. IPV advection at 00 UTC 4 Oct 1988 for (A) 310 K and (B) 320 K.
Positive/negative IPV advection (contour intervals 0.7 for (A) and 0.6 for (B)
$10^4 Ks^{-4}mb^{-1}$) are indicated by H/L, the position of Typhoon Nelson is indicated by
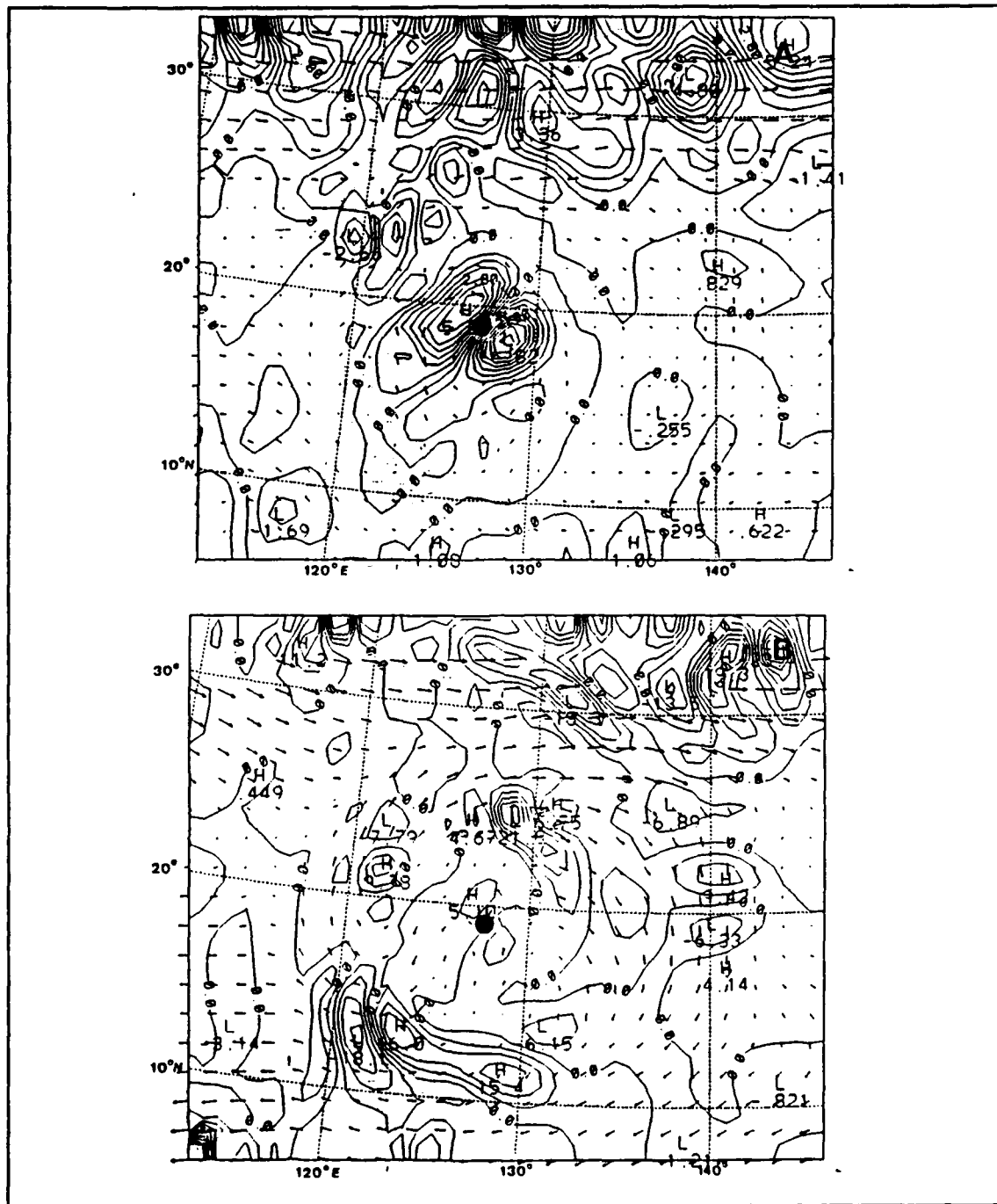the dot and the wind speeds are propotional to the vector lengths.

Figure 19.   As in Fig. 18, except for 00 UTC 4 Oct 1988 at (A) 340 K and (B) 350 K.   Contour intervals are 0.7 for (A) and 4 for (B)

as two minima occur. Nevertheless, self-advection is likely the key process influencing the propagation of the storm.

At 340 K (Fig. 21a), other IPV advection features are apparent. Significant positive and negative IPVA centers are located to the northeast of the vortex. Later analyses (not shown) indicate that these lobes are transient in nature and therefore are of little significance in storm propagation.. The two lobes near the storm center have become extremely distorted as each lobe now has two centers. It would be difficult to determine the vortex motion from this IPVA pattern. The "wobble" of the upper-level maxima described earlier is probably related to this complex IPVA pattern.

The effects of the bogus vortex on the IPVA pattern at 350 K has decreased in 12 h (Fig. 21b). Although the pattern still shows some distortion, the lobes of positive and negative IPVA are not as numerous as is in the initial pattern (Fig. 19b). The dominant upper-level IPVA near the vortex shows very little change from the preceding analysis.

Significant advection maxima other than those associated with the vortex are first detected at 1200 UTC 5 October 1988 (Fig. 22a). A dipole of positive and negative IPVA centers is found to the northeast of the vortex and is probably due to the large-scale synoptic flow. The dipole pattern associated with the vortex indicates a north-northwest propagation at this time, which agrees with the predicted track. At 320 K (Fig. 22b), the IPVA maxima are more distorted. The maximum value of IPVA is almost directly north of the storm center and two minima occur, one south of the center and the other to the southeast. Consequently, the orientation of the propagation vector is not well established at this level. However, the extension of the positive IPVA toward the north and northeast suggests continued recurvature. In the terminology of Sherman (1988), this would be a "primary node" toward which the storm would propagate.

By 0000 UTC 6 October 1988, the advection field has become more complicated (Fig. 23a). The centers of positive and negative IPVA near the vortex are still apparent. However, other centers have developed to the north and northwest of the vortex. The dipole to the northwest is due to a propagating shortwave. The negative lobe to the north contributes to a "wavetrain" pattern oriented along the general synoptic flow. This maximum/minimum pattern to the northeast may be a key indication of the recurvature of the storm. This pattern is also apparent at 320 K (Fig. 23b). The positive/negative wavetrain of IPVA to the northeast of the vortex may be a precursor of the subsequent storm movement to the northeast. Since this is only a single case study, the general applicability of this feature must be determined from many more cases.

Figure 20.   As in Fig. 18, except for 12 UTC 4 Oct 1988 at (A) 310 K and (B) 320 K.   Contour intervals are 0.6 for (A) and 0.6 for (B).

Figure 21. As in Fig. 19, except at 12 UTC 4 Oct 1988 for (A) 340 K and (B) 350
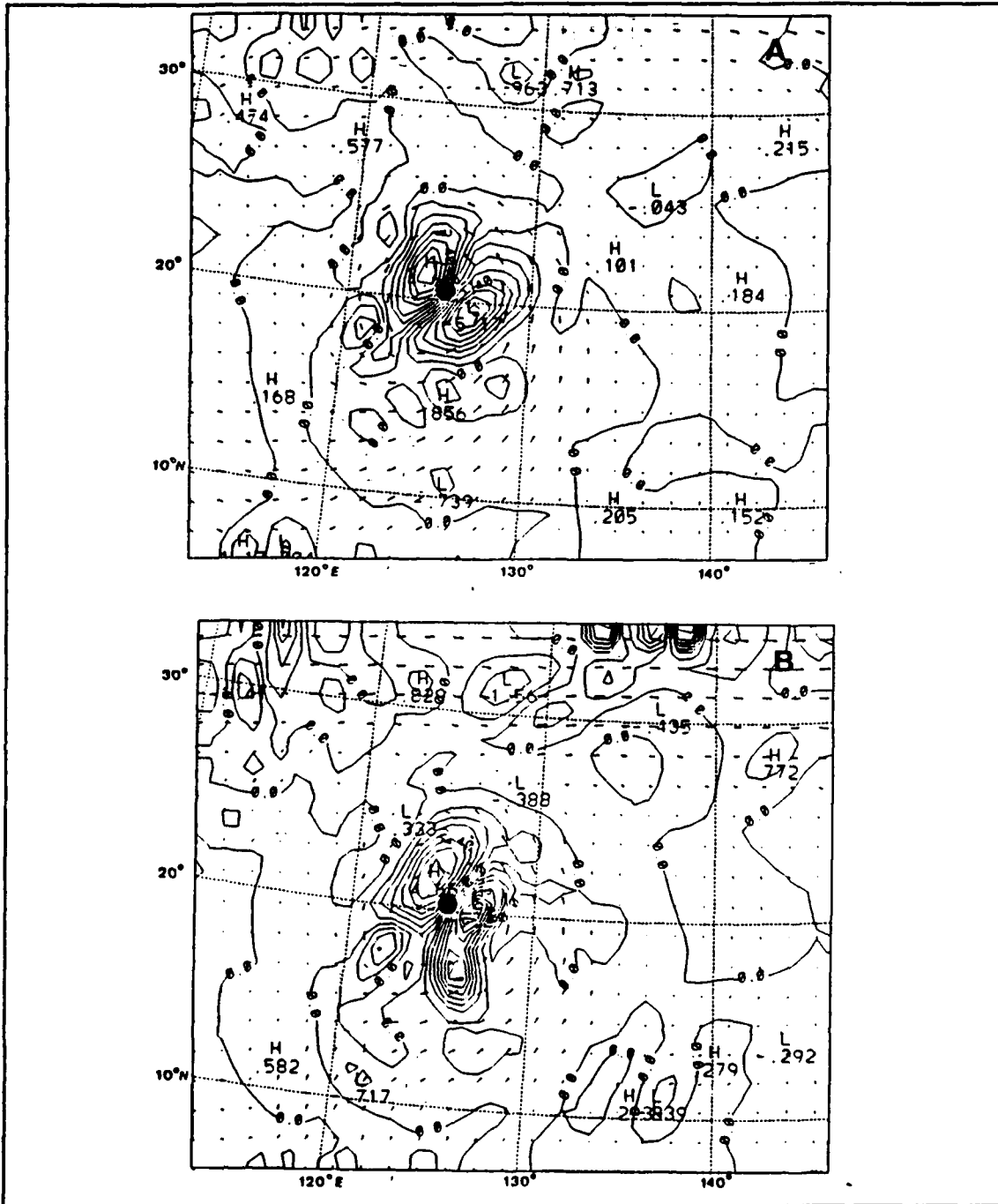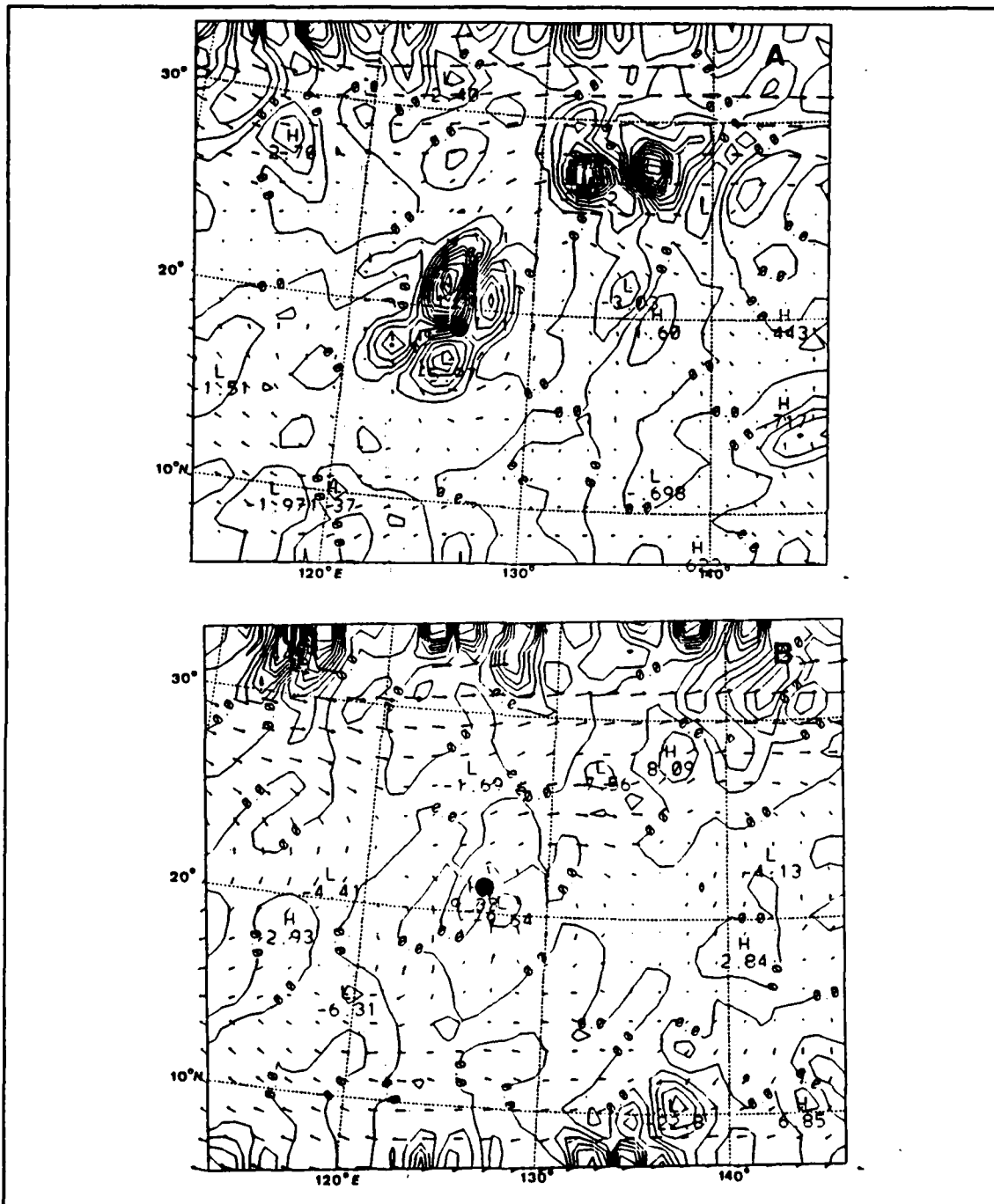K. Contour intervals are 1 for (A) and 5 for (B).

Figure 22. As in Fig. 18, except at 12 UTC 5 Oct 1988 for (A) 310 K and (B) 320 K. Contour intervals are 1 for (A) and 1 for (B).

40

Figure 23.   As in Fig. 18, except at 00 UTC 6 Oct 1988 for (A) 310 K and (B) 320 K.   Contour intervals are 1 for (A) and 2 for (B).

At 1200 UTC 6 October 1988, the centers of positive and negative IPVA are still found to the northeast of the storm (Fig. 24a) as in the pattern 24 h previously. The positive and negative centers of IPVA associated with the short wave are also readily apparent in this figure. This wave continues to propagate to the southeast. At 320 K (Fig. 24b), the short-wave and the large-scale feature to the northeast of the vortex are not well represented.

At the final time (Fig. 25a), the configuration of the 310 K pattern with repect to the vortex has not changed significantly in 12 h. A large center of negative IPVA is situated to the northeast of the storm center. Although the tropical cyclone is deeply embedded in the large-scale flow, the dipole associated with the vortex shows very little distortion. The shortwave to the west of the storm is not well organized as it continues to propagate to the southeast. A similar orientation of the IPVA is found at 320 K (Fig. 25b). The large-scale orientation to the northeast is more apparent as the negative IPVA center interacts with the IPVA dipole associated with the tropical cyclone.

In summary, significant changes are revealed in the IPVA fields as the storm evolves from the initial analysis to the forecast fields after 72 h. Self-advection was initially the major influence on storm movement, and adjacent advective features only appear at later times. The significance of these features and their role in storm propagation can be determined only by further study.

The transmission of these IPV fields along with the NORAPS track forecast may contribute to the understanding of the dynamical processes involved in storm propagation. Such fields could contribute to the decision of whether the recurvature forecast of the tropical cyclone is synoptically consistent and thus should be accepted.
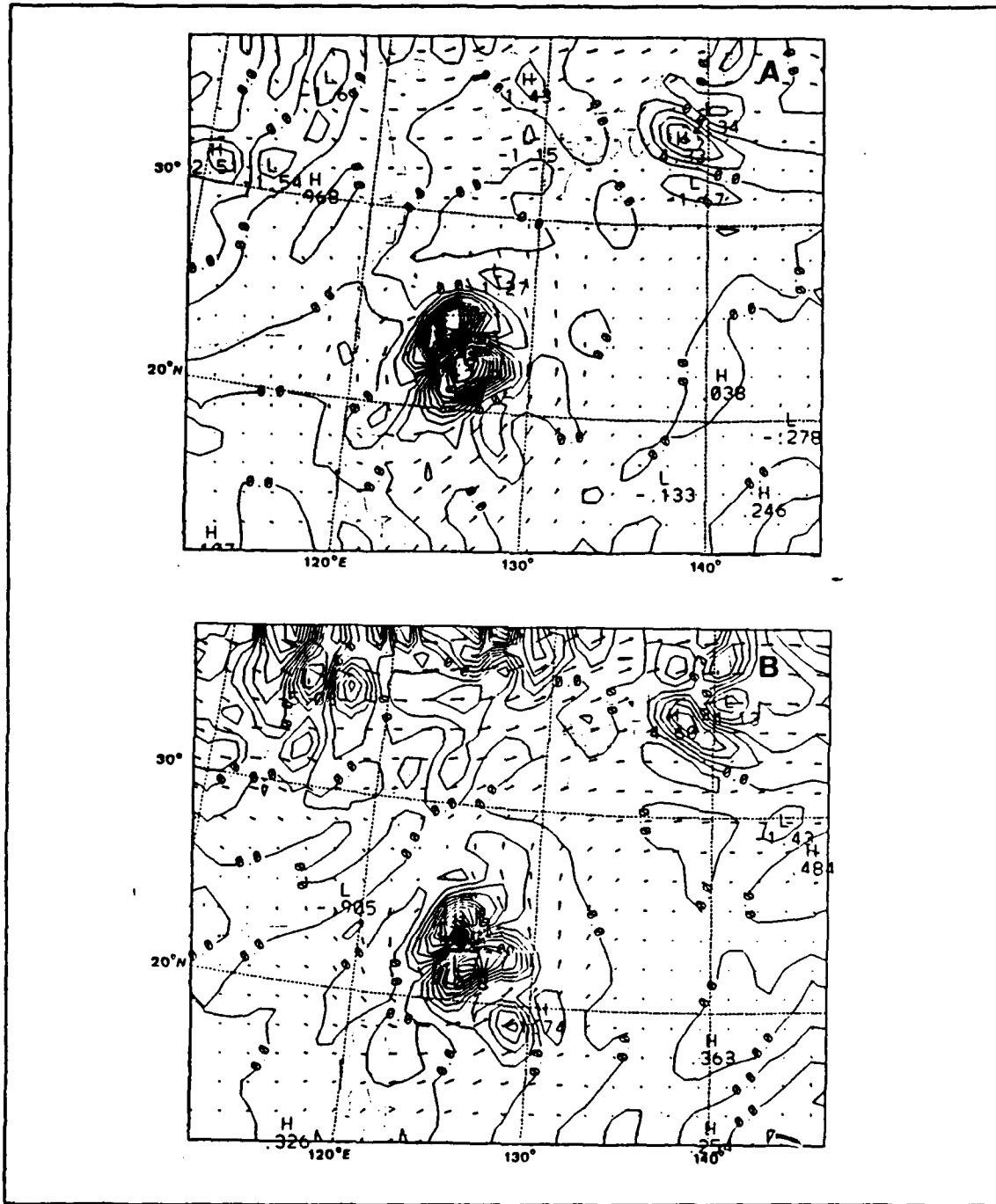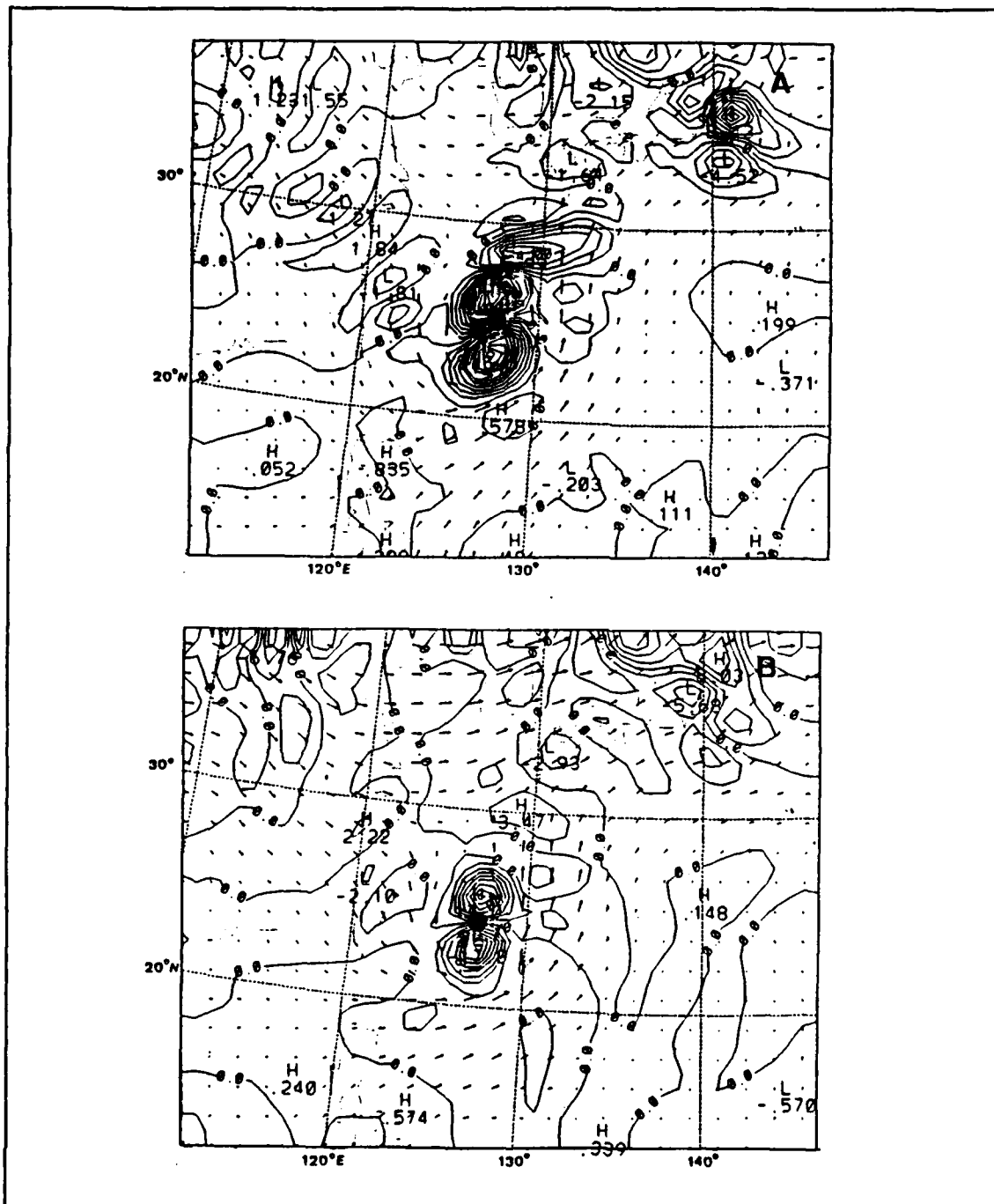
Figure 24. As in Fig. 18. except at 12 UTC 6 Oct 1988 for (A) 310 K and (B) 320 K. Contour intervals are 1 for (A) and 2 for (B).
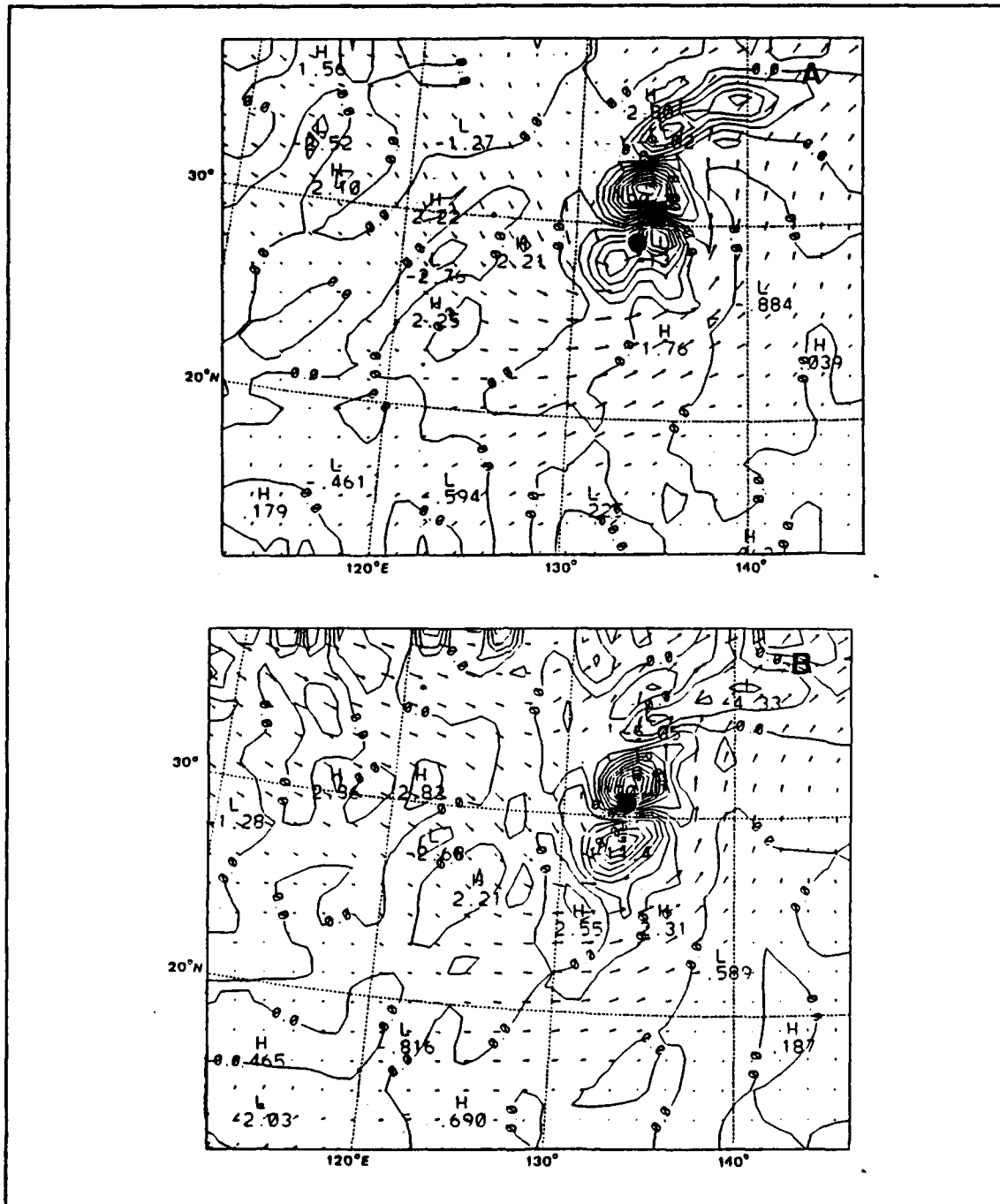
43

Figure 25.   As in Fig. 18, except at 00 UTC 7 Oct 1988 for (A) 310 K and (B) 320
K.   Contour intervals are 2 for (A) and 2 for (B).

44

V. CONCLUSIONS

The purpose of this study is to determine the feasibility of using model-generated isentropic potential vorticity (IPV) fields to aid in the forecast of tropical cyclone movement. The IPV fields are from the NORAPS forecast of Typhoon Nelson in the period 0000 UTC 4 October to 0000 UTC 7 October 1988. The fields are analyzed every 12 h.

Various researchers have made use of the distribution and structure of IPV fields in their attempt to explain midlatitude phenomena such as cyclogenesis and explosive cyclogenesis. The major deficiency in these studies is the lack of horizontal and vertical resolution due to the sparsity of observations in the area of interest. This is also a major concern in tropical analysis where few rawinsondes exist. To overcome this obstacle, researchers have used numerical models. However, most operational numerical models do not have adequate vertical resolution to describe key IPV features. NORAPS was selected for this study because its vertical (21 levels) and horizontal (80 km) resolution should be sufficient to adequately describe these features.

A synoptic analysis of Typhoon Nelson using NOGAPS 300 and 500 mb height fields is used first to determine if Nelson interacted with a midlatitude cyclone. However, the interaction appears to occur on horizontal scales too small to be accurately represented by synoptic-scale data. The motivation for using model-generated fields is that these "gaps" in data are avoided.

The analysis of IPV fields in Typhoon Nelson illustrates how the over-sized bogus vortex distorts the IPV fields and possibly degrades the storm forecast. The model evidently responds to negative IPV values on the periphery of the large bogus via inertial instability. An uncoupling of the upper and lower levels may be due to the inability of the model to sustain the bogus vortex. The over-sized bogus may lead to a degradation in the model forecast as it takes the model approximately 36 h to adjust to the initial imbalance in the mass and wind fields.

The IPV advection patterns are examined to determine if the calculations of these fields may aid the forecaster in isolating the key features governing tropical cyclone movement. Significant changes in the IPVA fields are found as the storm evolved from the initial analysis to the forecast field 72 h later. Initially, self-advection due to the orientation of the positive and negative dipoles near the storm center is the dominating

45

factor in the storm movement. After a 36 h integration, other adjacent advective features become apparent.

In future research, IPV fields for additional tropical cyclones undergoing recurvature should be analyzed. The general applicability of the interaction of IPV fields and their apparent effects on storm propagation in this case study then can be determined. Another illustration of the significance of these interactions is to modify the initial NORAPS fields so that the tropical cyclone is displayed southward from the initial position. An examination of the differences in the IPV interactions when the modified storm does not recurve should indicate the IPV effects to distinguish between recurvature and non-recurvature.

An effort must be made to improve the bogus structure. A bogus vortex that better represents the actual size of the tropical cyclone is needed, especially in the upper levels. A better representation of the vortex should reduce the time required for the model to adjust to the imbalance in the mass and wind fields. A realistic bogus thus may improve the early portion of the model forecast.

Finally, an effort must be made to transmit dynamical fields, such as IPV, to the forecasters. An enhancement of the forecaster's dynamical knowledge will lead to improvements in tropical cyclone forecasts.

APPENDIX A. NAVY OPERATIONAL REGIONAL ATMOSPHERIC PREDICTION SYSTEM

NORAPS was developed by Dr. Rich Hodur of the Naval Environmental Prediction Research Facility (NEPRF). The purpose of NORAPS is to provide a high resolution forecast of up to 42 h for those areas which are of importance to military operations. Since 1987 NORAPS has been used as a tropical cyclone track prediction model in the western North Pacific Ocean. This has been accomplished by artificially incorporating tropical cyclone(s) into the NORAPS initial fields and tracking their positions during the forecast (Hodur 1988).

The major advantage that NORAPS has over global or hemispheric models is the capability to resolve very small spatial features. Another key attribute of NORAPS is its flexibility. NORAPS is designed to be used anywhere in the world with a globally relocatable grid. The user has the ability to specify the dimensions and the horizontal/vertical resolution. An additional feature of NORAPS is the "terrain enveloping" concept in which topography is calculated at a high horizontal resolution so as to incorporate the effects of the sub-grid scale features into the topography field. A more indepth discussion of NORAPS is provided by Hodur (1982, 1987).

NORAPS consists of four major components: analysis, initialization, forecast and output. In the analysis, NORAPS includes a regional analysis of wind, temperature and D values. In the operational version described by Hodur (1987), first-guess values are obtained by interpolating Navy Operational Global Atmospheric Prediction System (NOGAPS) fields with a bicubic spline to the NORAPS forecast domain. Sea-level pressure and sea-surface temperatures obtained from the Fleet Numerical Oceanography Center (FNOC) are also incorporated into the analysis. These two analyses are run independently of NORAPS and NOGAPS.

NORAPS now uses a regional multivariate optimum interpolation (OI) scheme using 15 pressure levels (R. Hodur 1988). This method is based on the work of Lorenc (1981) and includes a second-order autoregression function as the forecast error correlation function. The incorporation of the OI scheme is a departure from the operational version of NORAPS as described by Hodur (1987). Another modification to the operational version is the use of a new initialization phase. The research version used in this

study incorporates a nonlinear vertical mode initialization as described by Bourke and McGregor (1983).

Rawinsonde, aircraft, ship and pibal data, as well as satellite soundings are used in the analysis procedure. Hodur (1987) states that satellite data are used exclusively over the ocean. All observation types are weighted equally in the wind analysis, whereas rawinsonde data are weighted three times larger than all other data types in the mass analysis.

The forecast component is the main driving force of NORAPS and requires the majority of the computer time. NORAPS uses the flux form of the primitive equations on a staggered grid scheme C as described by Arakawa and Lamb (1977). The vertical structure of the grid is shown in Fig. 26 and the horizontal stucture is shown in Fig. 27. All of the prognostic variables (u, v, q and T) are located at the middle of each layer, and the diagnostic vertical velocity is at the sigma level. The model uses sigma as the vertical coordinate, which orients all coordinate surfaces parallel to the terrain surface. Sigma is defined as the pressure at any height divided by the surface pressure. The research version of the forecast model uses 21 sigma levels (Table 1) instead of the 12 levels described by Hodur (1987).

The time integration scheme in the forecast model is a split-explicit technique developed by Madala (1981). Even though this scheme allows for longer time steps for the slower meteorological modes, it still has the ability to predict all of the gravity modes. The specific size of the time step is governed by the computational stability criterion for the horizontal resolution selected. All of the equations in the model are solved using a centered time (leapfrog) and space differencing scheme. Fourth-order advection is used in all of the equations.

Hodur (1987) states that fourth-order diffusion is used in all the prognostic equations, except that second-order diffusion is used on the first interior row. The diffusion is done on the sigma levels, which has a tendency to lead to spurious sources and sinks of energy when applied to the mass and moisture fields. This problem is alleviated by applying diffusion to deviations from the standard atmosphere for the temperature, moisture and pressure. The diffusion coefficient is then computed in the following manner

$$K_h = \frac{5\nabla x}{3} \qquad (A-1)$$
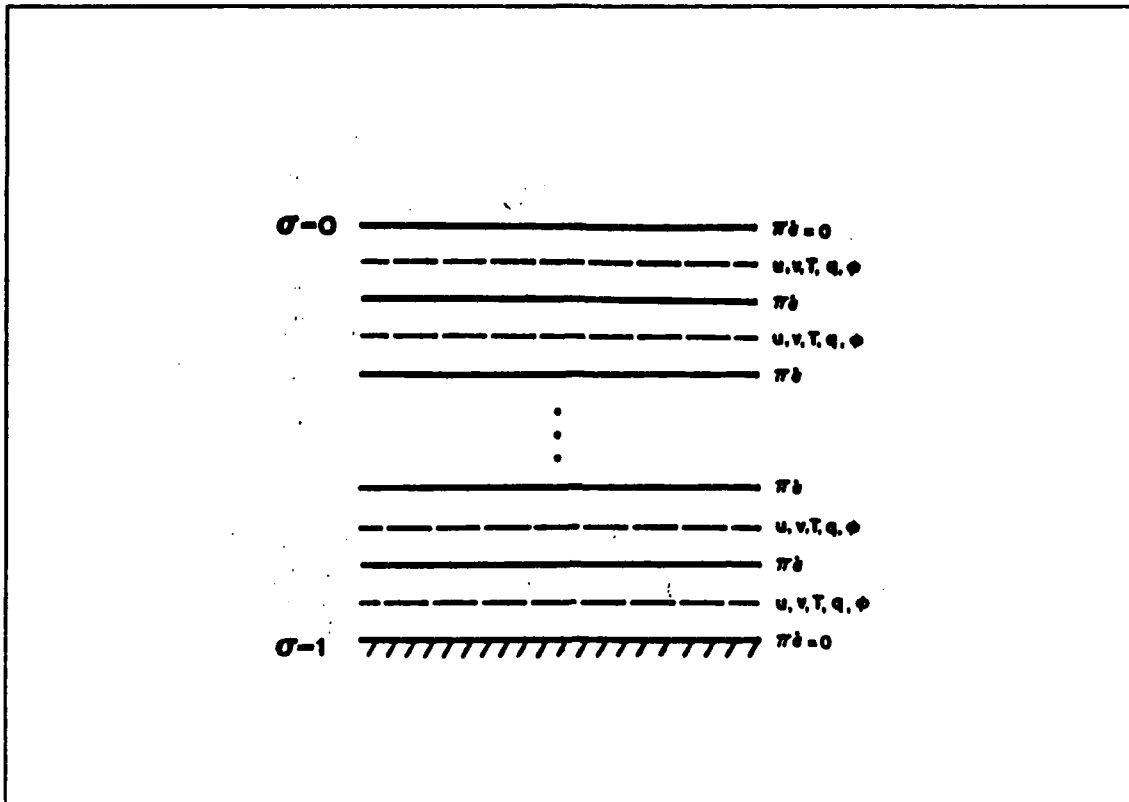
on the first interior row and

Figure 26. Vertical structure of the NORAPS sigma surfaces with distribution of variables (Hodur 1987).

$$K_h = -1.25\nabla x \qquad\qquad (A - 2)$$

on all other interior points, where ∇x is the grid spacing in meters. A Robert filter with a smoothing coefficient of 0.15 is then applied to control the high frequency time oscillations.

The NORAPS model uses one-way influence boundary conditions that specify the time-dependent lateral boundary values on the finer mesh NORAPS model from the NOGAPS predictions. Although the NOGAPS solution forces the fine-mesh model, the fine grid has no effect on the coarse-grid solution. Because of timeliness restrictions due to operational restraints, the boundary conditions are acquired from the previous 12-h forecast. A scheme developed by Perkey and Kreitzberg (1976) is used to spatially interpolate the solutions near the boundaries of the NORAPS model. The NOGAPS time tendencies are combined with the NORAPS time tendencies over a distance of several

π u π u π

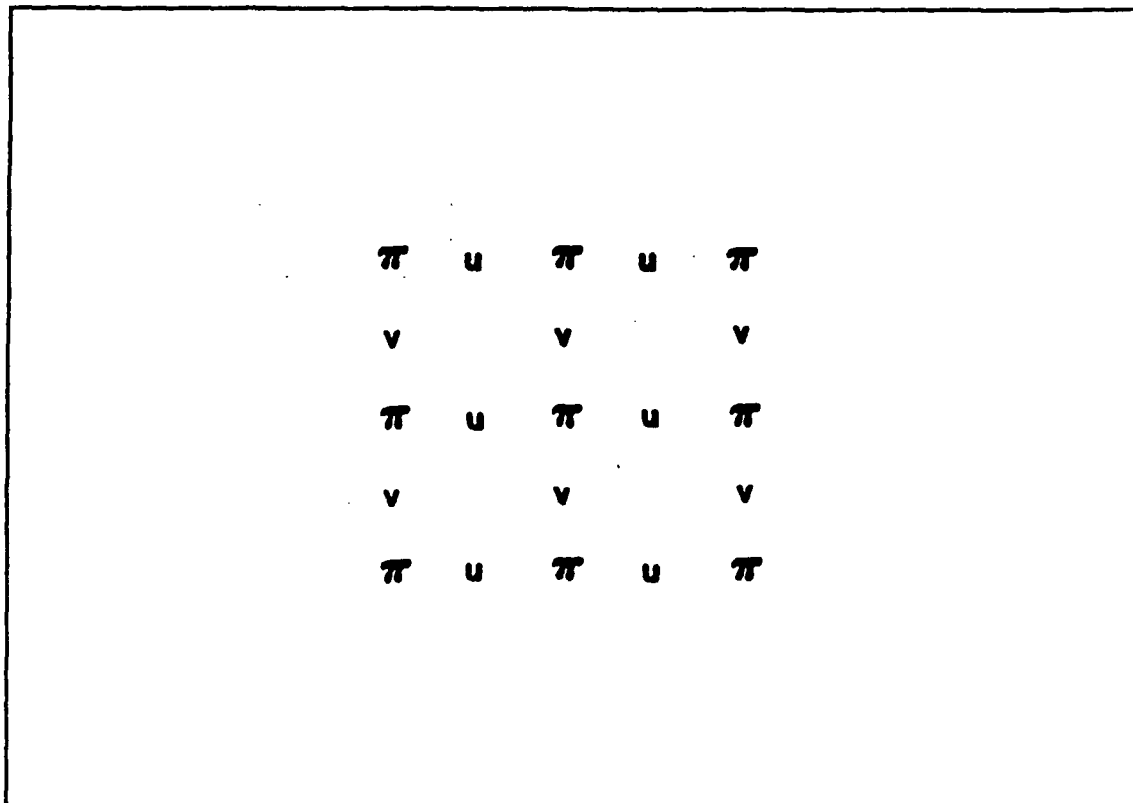v   v   v

π u π u π

v   v   v

π u π u π

Figure 27.   Horizontal structure of the NORAPS with distribution of variables (Hodur 1987).

grid points to reduce false reflections at the regional model boundary due to the change in grid spacing.

The numerical model would not be complete without some type of numerical simulation of the planetary boundary layer (PBL). The PBL is defined as the lowest layer in the model atmosphere and is well mixed in temperature, momentum and moisture. Interactions that occur between the PBL and the upper atmosphere provide sources and sinks for momentum, heat and moisture. According to Hodur (1988) NORAPS makes use of a multilayer PBL scheme that is based on Louis (1979) and is a change from the PBL scheme described by Hodur (1987).

According to Hodur (1987), the NORAPS uses a modified version of the Kuo (1965) cumulus parameterization method. This scheme links the convection to PBL variables by requiring moisture convergence in the PBL. The moisture convergence is defined as

$$M_t = \frac{1}{g} \nabla q_m \pi v_m \times (1 - \sigma_{PBL}) + \rho_s \overline{w' q'}_s, \qquad (A-3)$$

where the first term on the right side is the vertically-integrated moisture convergence and the second term is the surface moisture flux. Convection occurs when $M_t > 7.055 \times 10^{-7} gm^{-2}s^{-1}$ and when the equivalent potential temperature decreases with height from the PBL to the first layer above the PBL. The final constraint to this process is that the convection cannot occur if the lifting condensation level is above the PBL, which insures that the mixing is strong enough to force convection. This scheme separates the moisture transport into two parts, as described by Kuo (1974). A value of b is defined such that (bM_t) is used to moisten the environment and $(1 - b)M_t$ condenses and falls instantaneously as rain. The factor b is defined as the vertical average of $1 -$ relative humidity (RH), where RH is defined between 0 and 1. Introduction of the factor b tends to moisten the column more for a low RH and to condense more moisture for a high RH. The modified Kuo scheme provides only the physics of convective precipitation, but does not describe large scale (non-convective) precipitation.

Non-convective precipitation is assumed to occur when supersaturation conditions occur at a gridpoint. Moisture is condensed until saturation is reached, and the condensed moisture falls into the next layer below and will evaporate until saturation occurs. If the layer below is already super-saturated, the moisture will continue to fall to the next layer. Thus, precipitation will occur only if the air is saturated from the cloud to the ground. The precipitation routines are called every eight time steps, which enhances computer efficiency. The heating and moistening rates are then spread evenly over the subsequent eight time steps.

The NORAPS forecast model also takes into account solar radiation, which is essential in the prediction of surface temperatures, and calculates cooling rates of cloud tops that may deepen cloud layers. The radiation parameterization in the NORAPS model follows Katayama (1974) for short-wave radiation and Sasamori (1968) for long-wave radiation.

The final component of NORAPS is the output of the forecast fields for use by the forecaster. Data can be interpolated to 15 pressure levels. Recent changes in the model have improved the resolution below 850 mb and above 100 mb. Output parameters include winds, temperature, surface pressure, relative humidity, absolute vorticity and latent heat release. The forecaster has the option of using Mercator, Lambert conformal

51

or stereographic projections, which helps minimize distortions in the tropics, midlatitudes or polar regions, respectively.

A bogus vortex has been incorporated into the NORAPS due to the relative lack of data in the vicinity of tropical cyclones (Hodur 1988). The bogus vortex is derived from a model-generated storm produced by integrating NORAPS to a steady-state from an initially symmetric circulation, with a constant sea-surface temperature and a no-mean flow environment. The gridpoints from this forecast are used as observations in a successive-correction analysis to incorporate the storm structure into the initial fields. These model observations are dominant within 800 km of the center and are linearly reduced to zero at 1600 km. A heirarchy of storms have been generated based on the initial latitude. The spin-up storm that most closely matches the latitude of the storm is selected for the bogus. Prior to the 1988 season, a change was made to use the beta-plane rather than the f-plane in the model-generated storm (Hodur 1989).

Table 1. NORAPS MODEL SIGMA LEVELS.

Level number	Original sigma values	Intermediate sigma values
1	.02	.01
2	.05	.035
3	.085	.675
4	.125	.105
5	.175	.15
6	.225	.20
7	.275	.25
8	.325	.30
9	.375	.35
10	.450	.4125
11	.550	.50
12	.650	.60
13	.750	.70
14	.825	.7875
15	.875	.85
16	.905	.89
17	.935	.92
18	.965	.950
19	.985	.975
20	.995	.990
21	1.00	.9975

APPENDIX B.   DATA ACQUISITION AND PROCESSING

A.   DATA ACQUISITION

The NORAPS analysis and forecast fields were obtained from Dr. Rich Hodur of the Naval Environmental Prediction and Research Facility (NEPRF).   Data from the 9-track tape were transferred to a mass storage device on the Naval Postgraduate School (NPS) IBM 3033 computer.   The data fields are on a 79 × 69 staggered C-grid with 21 sigma levels.   Sigma is the vertical coordinate used by the model and is defined as $\sigma = \frac{p}{p_s}$, where p is the pressure at any height and p_s is the terrain pressure.   Sigma is defined as 1 at the surface where $p = p_s$ and zero at the top of the model where $p = 0$. The horizontal grid spacing used in the model is 80 km.   The analysis time for the model forecast is 0000 UTC 4 October 1988.   A 72-h forecast is generated with output fields available every 12 h until 0000 UTC 7 October 1988.

The NORAPS model output fields are on a Lambert conformal projection.   This scheme is a bi-conic, secant type of projection that preserves angles when projecting the earth's surface onto a plane surface.   The Lambert conformal projection scheme is best suited for the midlatitudes due to the minimal distortion between the true parallels of 30° and 60°N.   When used in the tropics, this scheme produces distortion of land masses and representations of meteorological variables near the equator.   These deficiencies are alleviated by modifying the graphics display program used in this study.

The variables from the model forecast are the u and v wind components, temperature, specific humidity, terrain pressure, mean sea-level pressure and ground temperature.   Along with these variables, the forecast fields also include the surface sensible heat flux, surface latent heat flux, convective and stable precipiatation.

Manipulations of the variables were performed on the NPS IBM mainframe computer.   The results were then transferred to main storage device on the NPS Meteorology/Oceanography Interactive Digital Environmental Analysis (IDEA) Laboratory.   It was decided to make use of the IDEA lab due to the availability of display programs designed by Prof. Wendell Nuss, Dept. of Meteorology.

B.   DATA PROCESSING

The concept of isentropic potential vorticity is based on the conservation of potential vorticity for air flow on a theta surface (Hoskins et al. 1985).   Potential vorticity may

change due to latitudinal displacements (Coriolis parameter) or by diabatically changing the separation of the isentropic layers.

Potential vorticity is computed on a three-dimensional array of grid points using the expression from Hoskins *et al.* (1985)

$$IPV = g \times \left([\zeta_p + f] \frac{\partial \theta}{\partial p} - \frac{\partial v}{\partial p} \frac{\partial \theta}{\partial x} + \frac{\partial u}{\partial p} \frac{\partial \theta}{\partial y} \right), \qquad (B-1)$$

where IPV is the potential vorticity on an isentropic surface, ζ_p is the relative vorticity on a constant pressure surface, f is the Coriolis parameter, θ is the potential temperature, p is the pressure and u and v are the zonal and meridional wind components. The last two terms on the right side of the equation are necessary for the coordinate transformation from pressure to isentropic coordinates. Because the NORAPS output uses sigma as the vertical coordinate, another coordinate transformation must be incorporated into $(B-1)$. The transformation from pressure to sigma coordinates was computed using the following identities as described by Phillips (1957),

$$\frac{\partial v}{\partial p} = \frac{1}{P_s} \frac{\partial v}{\partial \sigma}, \qquad (B-2)$$

$$\frac{\partial u}{\partial p} = \frac{1}{P_s} \frac{\partial u}{\partial \sigma} \quad \text{and} \qquad (B-3)$$

$$\frac{\partial \theta}{\partial p} = \frac{1}{P_s} \frac{\partial \theta}{\partial \sigma}. \qquad (B-4)$$

Using these identities, IPV was calculated on an isentropic surface from the sigma surface fields.

The NORAPS model output is on a staggered C-grid. The major disadvantage of this scheme for calculating IPV is that the u and v wind components are not located at the same gridpoint. An averaging technique is used to define values of u (v) to the north-south (east-west) of a central gridpoint where θ is defined

$$UMEAN(I, J) = \frac{u(I-1, J) + u(I, J) + u(I-1, J+1) + u(I, J+1)}{4} \qquad (B-5)$$

which gives a mean value of u at the original v gridpoints. A similiar procedure is used to define the mean v component for the east-west derivative. The values of $\frac{\partial u}{\partial y}$ and $\frac{\partial v}{\partial x}$ are then used in

$$\zeta_p = \frac{\partial v}{\partial x} - \frac{\partial u}{\partial y} \qquad\qquad (B-6)$$

to compute the relative vorticity. The values of relative vorticity at each sigma level are then vertically averaged to give a value of ζ_p at a point between two successive sigma levels. This is required because $\frac{\partial \theta}{\partial p}$, $\frac{\partial u}{\partial p}$ and $\frac{\partial v}{\partial p}$ are calculated between sigma surfaces. Therefore, IPV is also calculated at an intermediate level between two sigma levels.

Six theta surfaces are examined to describe the key features for this study. A major consideration is to assure that the vertical resolution is fine enough so that even small values of IPV can be accurately determined. By using 21 sigma levels and then transforming to theta surfaces, a more detailed representation of IPV is achieved. This is a major advantage over earlier IPV studies in which mandatory pressure levels were used (Elsberry and Kirchoffer 1988). Detailed structures may be lost due to the decrease in vertical resolution.

A linear interpolation scheme is used to transform the coordinate system from sigma to theta surfaces. A theta search is defined with values ranging from 300 to 360 K. The theta search value is bracketed between two sigma levels at each grid point. The u and v wind components, pressure and IPV are then interpolated linearly at the defined sigma surface. The value of these variables corresponds to a specific theta surface at each grid point. Using the IDEA Lab and the programs designed by Prof. Nuss, these variables are plotted on horizontal theta surfaces. Vertical cross-sections also are used to illustrate the vertical structure of these variables in the model analysis and forecast.

LIST OF REFERENCES

Abbey, R. F., Jr., and R. L. Elsberry, 1989: Progress and plans for the Office of Naval Research tropical cyclone motion initiative. 18th Conference on Hurricanes and Tropical Meteorology, Amer. Meteor. Soc., Boston MA, 02108, 235 pp.

Arakawa, A., and V. R. Lamb, 1977: Computational design of the basic dynamic process of the UCLA general circulation model. *Methods in Computational Physics*, 111, Academic Press, 173-265.

ATCR, 1988: Annual Tropical Cyclone Report. NAVOCEANCOMCEN/JTWC, COMNAVMARIANAS Box 17, FPO San Francisco, CA, 96630, 216 pp.

Bourke, W., and J. L. McGregor, 1983: A nonlinear vertical mode initialization scheme for a limited area prediction model. *Mon. Wea. Rew.*, 111, 2285-2297.

Ciesielski, P. E., D. E. Stevens, R. H. Johnson and K. R. Dean, 1989: Observational evidence of asymmetric inertial instability. *J. Atmos. Sci.*, 46, 817-831.

Danielsen, E. F., 1968: Stratospheric-tropospheric exchange based on radioactivity, ozone and potential vorticity. *J. Atmos. Sci.*, 25, 502-518.

Eliassen, A., 1952: Slow thermally or frictionally controlled meridional circulation in a circular vortex. *Astrophys. Norv.*, 5, 60 pp.

Elsberry, R.L., 1987: *A Global View of Tropical Cyclones*. Office of Naval Research Marine Meteorology Program, 185 pp.

_____, and P. J. Kirchoffer, 1988: Upper-level forcing of explosive cyclogenesis over the ocean based on operationally analyzed fields. *Wea. and Forecasting*, 3, 205-216.

Hodur, R. M., 1982: Description and evaluation of NORAPS: The Navy Operational Regional Atmospheric Prediction System. *Mon. Wea. Rev.*, 110, 1591-1602.

_____, 1987: Evaluation of a regional model with an update cycle. *Mon. Wea. Rev.*, 115, 2707-2718.

_____, 1988: Tropical cyclone track prediction in a regional model. Preprints, Eighth Conference on Numerical Weather Prediction, Feb. 22-26, 1988, Baltimore, MD, Amer. Meteor. Soc. Boston MA, 02108, 585-590.

_____, 1989: Tropical cyclone track prediction in a regional model. 18th Conference on Hurricanes and Tropical Meteorology, Amer. Meteor. Soc., Boston MA, 02108, 235 pp.

Hoskins, B. J., M. E. McIntyre and A. W. Robertson, 1985: On the use and the significance of isentropic potential vorticity maps. *Quart. J. Roy. Meteor. Soc.*, 111, 877-946.

Katayama, A., 1974: A simplified scheme for computing radiative transfer in the troposphere. Tech Rep. *No. 6*, Dept. Meteor., UCLA, 77 pp.

Kuo, H. L., 1965: On formation and intensification of tropical cyclones through latent heat release by cumulus convection. *J. Atmos. Sci.*, **22**, 40-63.

___, 1974: Further studies of the parameterization of the influence of cumulus convection on the large-scale flow. *J. Atmos. Sci.*, **31**, 1232-1240.

Louis, J. F., 1979: A parametric model of vertical eddy fluxes in the atmosphere. *Boundary Layer Meteorology*, **17**, 187-202.

Lorenc, A. C., 1981: A global three-dimensional multivariate statistical interpolation scheme. *Mon. Wea. Rev.*, **17**, 187-202.

Madala, R., 1981: *Finite Difference Techniques for Vectorized Fluid Dynamical Calculations*. Springer-Verlag, 56-70.

Perkey, D. J., and C. W. Kreitzberg, 1976: A time-dependent lateral boundary scheme for limited-area primitive equation models. *Mon. Wea. Rev.*, **104**, 744-755.

Phillips, N. A., 1957: A coordinate system having some special advantages for numerical forecasting. *J. Meteor.*, **14**, 184-185.

Reed, R.J., 1955: A study of a characteristic type of upper-level frontogenesis. *J. Meteor.*, **12**, 226-237.

___, and F. Sanders, 1953: An investigation of the development of a mid-tropospheric frontal zone and its associated vorticity field. *J. Meteor.*, **10**, 338-349.

Sasamori, T., 1968: The radiative cooling calculation for application to general circulation models. *J. Appl. Meteor.*, **7**, 721-729.

Schubert, W. H., and B. T. Altworth, 1987: Evolution of potential vorticity in tropical cyclones. *Quart. J. Roy. Meteor. Soc.*, **37**, 994-1004.

Shapiro, M. A., 1980: Turbulent mixing within tropopause fields as a mechanism for the exchange of chemical constituents between the stratosphere and troposphere. *J. Atmos. Sci.*, **37**, 994-1004.

Sherman, B. T., 1988: Synoptic patterns related to tropical cyclone recurvature. M. S. Thesis, Naval Postgraduate School, 122 pp.

Thorpe, A. J. 1985: Diagnosis of balanced vortex structure using potential vorticity. *J. Atmos. Sci.*, **42**, 397-406.

Uccellini, L. W., D. Keyser, C. H. Wash and K. F. Brill, 1985: The Presidents' Day cyclone of 18-19 February 1979: Amplification and associated tropopause folding on rapid cyclogenesis. *Mon. Wea. Rev.*, **112**, 31-55.

INITIAL DISTRIBUTION LIST

12. Dr. G.J. Holland   1
    BMRC, P.O. Box 1289K
    Melbourne Vic 3001
    Australia

13. Dr. R. M. Hodur   1
    Naval Environmental Prediction
    Research Facility
    Monterey, CA 93943-5006

14. Dr. C.-S. Liou   1
    Naval Environmental Prediction
    Research Facility
    Monterey, CA 93943-5006

15. Dr. Ted Tsui   1
    Naval Environmental Prediction
    Research Facility
    Monterey, CA 93943-5006

16. Director   1
    Joint Typhoon Warning Center
    COMNAVMARIANAS Box 17
    FPO, San Francisco, CA 96630

17. Library Acquisitions   1
    National Center for Atmospheric Research
    P.O. Box 3000
    Boulder, CO 80307-5000

18. Director Naval Oceanography Division   1
    Naval Observatory
    34th and Massachusetts Avenue NW
    Washington, DC 20390

19. Commanding Officer   1
    Naval Oceanographic Office
    Stennis Space CTR, MS 39522-5001

20. Commanding Officer   1
    Naval Ocean Research and Development Activity
    Stennis Space CTR, MS 39529-5004

21. Chairman, Oceanography Department   1
    U. S. Naval Academy
    Annapolis, MD 21402

22. Chief of Naval Research   1
    800 N. Quincy Street
    Arlington, VA 22217